HHS Public Access

Author manuscript

J Am Chem Soc. Author manuscript; available in PMC 2020 July 30.

Published in final edited form as:

J Am Chem Soc. 2020 June 24; 142(25): 10964–10977. doi:10.1021/jacs.0c01671.

UvrC Coordinates an O_2-Sensitive [4Fe4S] Cofactor

Rebekah M. B. Silva, **Michael A. Grodick**, **Jacqueline K. Barton**

Division of Chemistry and Chemical Engineering, California Institute of Technology, Pasadena, California 91125, United States

Abstract

Recent advances have led to numerous landmark discoveries of [4Fe4S] clusters coordinated by essential enzymes in repair, replication, and transcription across all domains of life. The cofactor has notably been challenging to observe for many nucleic acid processing enzymes due to several factors, including a weak bioinformatic signature of the coordinating cysteines and lability of the metal cofactor. To overcome these challenges, we have used sequence alignments, an anaerobic purification method, iron quantification, and UV–visible and electron paramagnetic resonance spectroscopies to investigate UvrC, the dual-incision endonuclease in the bacterial nucleotide excision repair (NER) pathway. The characteristics of UvrC are consistent with [4Fe4S] coordination with 60–70% cofactor incorporation, and additionally, we show that, bound to UvrC, the [4Fe4S] cofactor is susceptible to oxidative degradation with aggregation of apo species. Importantly, in its holo form with the cofactor bound, UvrC forms high affinity complexes with duplexed DNA substrates; the apparent dissociation constants to well-matched and damaged duplex substrates are 100 ± 20 nM and 80 ± 30 nM, respectively. This high affinity DNA binding contrasts reports made for isolated protein lacking the cofactor. Moreover, using DNA electrochemistry, we find that the cluster coordinated by UvrC is redox-active and participates in DNA-mediated charge transport chemistry with a DNA-bound midpoint potential of 90 mV vs NHE. This work highlights that the [4Fe4S] center is critical to UvrC.

Graphical Abstract

Corresponding Author: Jacqueline K. Barton – Division of Chemistry and Chemical Engineering, California Institute of Technology, Pasadena, California 91125, United States; jkbarton@caltech.edu.
Complete contact information is available at: https://pubs.acs.org/10.1021/jacs.0c01671

Supporting Information

The Supporting Information is available free of charge at https://pubs.acs.org/doi/10.1021/jacs.0c01671.
Additional experimental methods; protein sequence regions containing putative LYR motifs; affinity and size exclusion chromatograms from purification; EPR spectra of ferric iron signals; SDS-PAGE, UV–vis spectra, and standard curve for molecular weight verifying that O_2 targets the [4Fe4S] center; selected data from early studies of UvrC; induction trials of C → A mutants; stability of UvrC in buffer containing a lower concentration of KCl; scan rate dependence of UvrC on DNA-modified Au electrodes; table of primers and substrates used in this study (PDF)

The authors declare no competing financial interest.

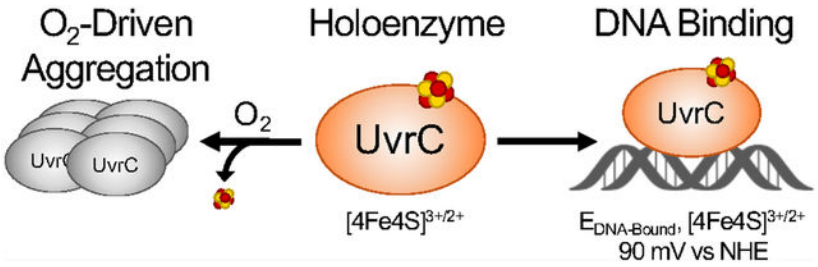

INTRODUCTION

Iron sulfur clusters are ubiquitous in proteins as inorganic cofactors found in all domains of life and are essential in major cellular processes, including respiration, photosynthesis, and nitrogen fixation.[1–5] In the past three decades, iron sulfur clusters have been found coordinated by many DNA repair and replication enzymes essential for genome maintenance.[6–11] In most of these proteins, however, the [4Fe4S] cofactor is not involved directly in catalytic activity on DNA substrates, so identifying a general role for the metal cofactor has become a growing area of interest.[12] Toward this end, we have investigated the DNA-bound redox chemistry of several repair and replication proteins and demonstrated that these proteins not only participate in DNA charge transport (DNA CT) chemistry but also do so at a shared potential of ~80 mV vs NHE, making electron transfer energetically favorable. We have found that the DNA-bound potentials of repair and replication proteins studied to date are consistent with those of high potential iron–sulfur proteins (HiPIPs).[12] Models have been developed to describe how redox signaling among repair proteins through DNA CT is utilized for rapid lesion detection and to explain how the oxidation of the cluster can act as a redox switch that modulates binding affinities to DNA substrates as well as processivity of eukaryotic replication polymerases.[13–15]

The observation of a [4Fe4S] cluster in repair and replication proteins has often occurred many years after the first characterization of the gene and gene products due to several reasons.[7,8,12] First, [4Fe4S] clusters, like other metal centers, can be sensitive to expression and purification conditions, which has delayed isolation of protein with intact clusters.[16–18] Second, prediction of [4Fe4S] coordination sites in nucleic acid processing enzymes has been particularly challenging because the spacing of the coordinating cysteines is atypical across different protein families, leading to a weak bioinformatic signature.[8] Other indications that a protein may bind an iron–sulfur cluster, such as the LYR sequence motif identified first in human protein sequences as a recognition element for iron–sulfur biogenesis machinery, are just emerging and could inform predictive tools for other organisms in the future.[17,19–21] In light of these reasons, several research groups have proposed that many more iron– sulfur cluster proteins involved in nucleic acid processing remain to be discovered.[7,16,17]

In *Escherichia coli* (*E. coli*), two repair glycosylases, Endonuclease III (EndoIII) and MutY, and one Superfamily 2 (SF2) 5′ → 3′ repair helicase, DinG, coordinate a [4Fe4S] cluster (a paralog of DinG, YoaA, has also recently been predicted to bind a [4Fe4S] cluster based on sequence similarity) and are active in essential repair pathways in prokaryotes.[22–28] EndoIII

and MutY primarily resolve oxidized pyrimidines and 8-oxoguanine mispaired with adenine, respectively, in Base Excision Repair (BER), while DinG is involved in resolving R-loops and D-loops (RNA or DNA or triple-stranded nucleic acid structures) which can occur at collisions between transcription and replication machinery.[29,30] Inexplicably, DinG overexpression and Δ*dinG* strains of *E. coli* are more sensitive to UV light, suggestive of redox signaling between DinG and an unknown protein in Nucleotide Excision Repair (NER; in eukaryotic and archaeal NER, XPD is known to a coordinate a [4Fe4S] center).[30,31] In prokaryotic NER, a relatively small pool of proteins recognize and repair structurally and chemically diverse bulky DNA lesions that arise due to DNA damage by UV light, cigarette smoke, small molecule chemotherapeutics, and protein–DNA adducts, among others.[32–34] In the classic model of bacterial NER, the UvrAB complex scans and searches the genome for bulky lesions, UvrC in complex with UvrB makes an incision 5′ and 3′ to the site of damage, UvrD unwinds the damaged oligomer, and DNA polymerase 1 and DNA ligase patch the damaged strand, completing the repair process (Figure 1).[32–34]

UvrC is unique in many respects among the proteins in the NER pathway, most notably in how challenging the protein has been to study, both *in vitro* and *in vivo*.[32–35] Insight on UvrC has been difficult to gain because of limited sequence homology to other proteins. UvrC comprises its own protein family of dual-incision endonucleases (also referred to as excision nucleases or exinucleases) with two distinct active sites located at the N and C termini of the same peptide.[33,36] UvrC has also been noted by many in the field to be difficult to purify and, once purified, to be susceptible to degradation, aggregation, and loss of activity over time, even when stored frozen.[34–36] Though first isolated in 1981, a full-length or near full-length crystal structure has not been reported for UvrC (in contrast to UvrA, UvrB, and UvrD), and cocrystal structures of UvrC in complex with a substrate or other NER proteins are also not available, which has limited searches for structural homology.[33,37,38] *In vivo* regulation of UvrC expression is complex and has been reported to be under the control of multiple promoters, which further distinguishes UvrC from the other proteins in the NER pathway.[39] Expression of radio-labeled UvrC was first reported to be 10–20 copies per cell, though subsequent studies of UvrC mRNA levels, fluorescently labeled UvrC, and active ribosomes have reported between 0.05 to 300 copies of UvrC per cell (or per cell per generation).[39–41] Furthermore, the expression of UvrC is not inducible by the SOS system, a cellular-wide response to DNA damage present in many bacteria.[42] This again is in contrast to UvrA, UvrB, and UvrD, which are induced during the SOS response.[43] In the context of repair proteins bearing a [4Fe4S] cofactor, tight regulation of copy number appears to be a common characteristic of these metalloproteins in *E. coli*.[12]

Our initial examination of UvrC began with the sequence of the protein. Five main regions of UvrC have been identified, which include the N-terminal GIY-YIG endonuclease domain (3′ incision), a cysteine rich region, a UvrBC interacting domain, the RNaseH endonuclease domain (5′ incision), and a helix-turn-helix motif (Figure 1).[33,34] In the N-terminal cysteine-rich region, four highly conserved cysteine residues at positions 154, 166, 174, and 178 have been observed. The function of the conserved cysteines has been unknown, but speculated to facilitate interactions between UvrB and UvrC.[34] Because the four cysteines are atypically spaced, close in proximity, and highly conserved through the Bacteria domain and up to some archaeal species ($CysX_{6–14}CysX_7CysX_3Cys$ consensus sequence), we hypothesized

that these cysteine residues coordinate a [4Fe4S] cluster (Figure 1). Two putative (LIV)(YF)(RK) tripeptide motifs were also observed (Figure S1), one of which is located N-terminal to the predicted coordination site and the other just after Cys154. Additionally, conserved aromatic and proline residues are also located around Cys154, Cys166, Cys174, and Cys178 (Figure S1), one of the few common themes among the sequences of nucleic acid processing enzymes that coordinate the [4Fe4S] cofactor.[8] More moderately conserved cysteine residues can be found at positions 265, 398, and 413, but these were not hypothesized to participate in Fe coordination because of the absence of other supporting sequence motifs suggestive of a [4Fe4S] binding domain.

Here, we report the discovery and characterization of a HiPIP-like [4Fe4S] cluster that is coordinated by UvrC. The holo form of UvrC is stabilized relative to its apo form; distinct from what has been reported to date for other [4Fe4S] repair proteins in *E. coli*, the cluster degrades in the presence of molecular oxygen. We also find, in its holo form, UvrC independently forms a high-affinity complex with DNA, though DNA binding does not lead to independent enzymatic activity on a damaged substrate. Finally, using DNA-modified Au electrodes, we observe that UvrC participates in DNA CT chemistry and shares a DNA-bound midpoint potential seen previously for EndoIII, MutY, and DinG. Based on these observations, we discuss UvrC activity in its holo form in the context of the NER pathway and the greater redox signaling network of [4Fe4S] repair proteins.

RESULTS AND DISCUSSION

Development of an Anaerobic Purification Method for UvrC.

UvrC has historically been difficult to express and purify.[32–35] Accordingly, we screened new expression and purification strategies that would yield soluble and pure protein in large enough quantities that a [4Fe4S] metal center could be detected spectroscopically. Included in the screen was a pBAD overexpression plasmid under the control of the L-arabinose promoter with a His_6-Maltose Binding Protein (MBP) affinity/solubility tag encoded N-terminally to UvrC (see Supporting Experimental Section).[44–47] The L-arabinose promoter can be used to prevent leaky expression prior to induction with arabinose, which is an advantage for overexpressing proteins that are potentially toxic to cells prior to induction.[48–51] Additionally, MBP tags are frequently used to enhance the expression and solubility of target proteins, including for previous overexpression of the C-terminal half of UvrC as well as repair and replication enzymes bearing the [4Fe4S] cluster.[52–58] A cooler overexpression temperature (22 °C), longer induction time (16 h), and an anaerobic purification in buffers that included a high concentration of potassium chloride were also chosen to minimize accumulation of apo, aggregated, or degraded protein.[7,11,17,59–65]

We found that the pBad overexpression system resulted in detectable overexpression of a His_6-MBP-UvrC fusion protein (110 kDa) in whole cell lysate (referred to as UvrC for the remainder of this manuscript, Figure S2). Cell lysis, purification, and concentration of the UvrC fusion protein using immobilized metal affinity and gel filtration chromatography was performed under strict anaerobic conditions in an anaerobic chamber and using a standard Schlenk line technique (Figure S2).[66,67] UvrC was concentrated between 20 and 30 μM to prevent precipitation after flash freezing in liquid N_2 and stored at −80 °C. The expression

and anaerobic purification strategy allowed for isolation of the UvrC fusion protein in high purity with a broad and shallow absorption band centered at 410 nm and yellow-tan color characteristic of a [4Fe4S] cluster (Figure 2).[3,68–70] Based on the ratio of absorbances at 410 and 280 nm, each purification yielded approximately 5 mg of the UvrC fusion protein per liter of liquid culture (5 g of wet pellet) with 60–70% incorporation of the [4Fe4S] metal center (Figure S2).[11,15,24,61,70–81] To characterize the nature of the Fe center further, we used the ferene colorimetric assay to quantify the amount of protein-bound Fe.[80] We find that UvrC coordinates about 3 Fe per protein on average (or 4.0 ± 0.3 Fe per cluster, Figure 2 and Figure S2), which is consistent with the substoichiometric levels of [4Fe-4S] cluster incorporation seen with other repair and replication enzymes. A range from 2 to 4 Fe per protein has been reported and has been attributed to incomplete incorporation or loss of a labile Fe during the process of overexpression or purification, even when each step is completed anaerobically.[25,27,53,61,64,82–85]

Holo-UvrC Is Redox-Active.

We used X-band electron paramagnetic resonance (EPR) spectroscopy to assign oxidation states of the [4Fe4S] cluster. A small signal centered at $g = 2.01$ can be seen from the native UvrC EPR spectrum, which has been observed previously and found to be due to a small percentage of the native protein population in the $[3Fe4S]^{1+}$ state (with the rest of the population in the EPR-silent $[4Fe4S]^{2+}$ state) (Figure 2).[27,54,64,72,82] Two categories of protein-bound [4Fe4S] clusters are known: (i) ferredoxins which cycle between the 2+/1+ oxidization states and (ii) HiPIPs which cycle between the 3+/2+ oxidation states.[68,69,86] To classify the nature of the [4Fe4S] cluster, UvrC was treated with the oxidant potassium ferricyanide and immediately frozen in liquid N_2, which resulted in a large and sharp signal at $g = 2.01$.[27,53,61,82,83,85] We assign this signal to a $[3Fe4S]^{1+}$ species derived from an oxidized $[4Fe4S]^{3+}$ cluster, indicating that UvrC accesses the 3+/2+ redox couple. Equivalent spectra have been observed for EndoIII and homologues, repair proteins with [4Fe4S] clusters that are generally substantially more stable under aerobic conditions.[54] A corresponding signal at $g = 4.3$ can also be observed after treatment with ferricyanide, suggestive of a ferric species in solution (Figure S3) and consistent with the release of an iron atom from the $[4Fe4S]^{3+}$ species following oxidization.[87,88] No clear evidence of the $[4Fe4S]^{3+}$ species, characterized by a $g = 2.1$, before Fe loss was apparent.[3,68,69] Taken together, the data for UvrC are consistent with other DNA repair proteins and coordinates a HiPIP-like [4Fe4S] cluster.

The UvrC-Bound [4Fe4S] Cluster Is Susceptible to Oxidative Degradation.

Protein-bound Fe centers can serve multiple functions in the cell,[6,89–91] and the role(s) of the [4Fe4S] center are still being defined for repair and replication proteins. The [4Fe4S] cluster is not involved in active site chemistry on DNA substrates for the majority of repair and replication proteins,[12] though a role for reactivity with dioxygen (and other reactive species) and redox signaling are just emerging (*vide infra*). With regard to sensing reactive species, particularly dioxygen, part of the challenge is that a range of stabilities under aerobic conditions has been observed for repair and replication proteins, and more labile [4Fe4S] centers which require anaerobic expression and/or purification conditions to remain intact (and therefore detectable) have only recently been reported.[12] To investigate if the

[4Fe4S] cluster of UvrC sensitive to O_2 at a physiologically relevant temperature, we incubated UvrC in aerobic UvrC buffer (25 mM Tris-HCl, 0.5 M KCl, 20% v/v glycerol) at 37 °C and monitored the absorption band at 410 nm. We find that on the time scale of a UvrC activity assay (1 h), 20% of the cluster degraded after incubation at 37 °C, while complete degradation was observed after 4 h (Figure 3). We verified that the bleaching of the absorbance at 410 nm was due only to degradation of the [4Fe4S] center and not the peptide through gel analysis (Figure S4). Notably, anaerobic incubation of holo UvrC at 37 °C in the absence of O_2 does not result in degradation of the [4Fe4S] cluster (Figure S4). We also observe that binding to duplex DNA does not affect cluster degradation (see below for studies of UvrC–DNA complexes) (Figure S4). We emphasize here that, in order to detect the oxygen-driven degradation spectroscopically, concentrations of UvrC well above that of what is commonly found in an activity assay needed to be used. Our observations highlight the subtlety of handling a metalloprotein *in vitro* and the importance of carefully monitoring cofactor stability.

Because apo and holo forms of metalloproteins can have different oligomeric states, we compared holo- and apo-UvrC by analytical size exclusion chromatography.[6,89] Using a standard curve, we determined that holo-UvrC elutes at a volume consistent with protein migrating in dimeric form (Figure 3 and Figure S4). In contrast, apo-UvrC species elute at the void volume of the column, which corresponds to aggregates that would be greater than 600 kDa in mass (Figure 3). Such a sensitivity to O_2 has not been seen previously in repair proteins that coordinate a [4Fe4S] cluster.

The significance of our observations and findings of other investigators regarding how [4Fe4S] cofactor in EndoIII, MutY, DinG, and UvrC are transformed by exposure to reactive species remains to be explored fully *in vitro* and *in vivo*. As summarized above, EndoIII, MutY, and DinG have not been reported to be similarly sensitive to O_2. Moreover, we have observed previously that EndoIII is not only highly soluble but also stable at room temperature in atmosphere for many days. EndoIII, homologue MutY, and DinG have furthermore been crystallized aerobically.[58,74,80,92–94] EndoIII does, however, react rapidly with another diatomic signaling molecule, NO, causing loss of one iron atom per cluster and formation of a mononuclear dinitrosyl iron complex and a dinuclear Roussin's red ester in the cluster binding domain.[80] Transformation of the iron center is reversible and does not affect global protein structure or DNA binding, but does shift the redox potential of the cluster and hinders enzymatic activity.[80,95] DinG also reacts with NO and is inactivated, but surprisingly, is resistant to treatment with H_2O_2.[25] Cellular responses mediated by sensing of reactive species by iron– sulfur transcription factors has been well-characterized, though in contrast, the specificity and responses of repair proteins to reactive species are not as fully understood.[6] Variations in the stability of the [4Fe4S] cofactor from repair proteins across different bacterial species adapted to niche environments are also not fully appreciated.[33,96–99] Exploring how UvrC and other DNA repair enzymes are involved in detecting changes in cellular environments and in the cellular response to endogenous and exogenous stressors (separate or related to their repair activities in the genome) is an area that warrants further investigation.

As emphasized above, metalloproteins can be challenging to handle, and oxidative degradation of the [4Fe4S] cofactor of UvrC was nontrivial to observe. Our early studies were carried out with UvrC purified aerobically at 4 °C (Figure S5, top left).[100] The protein was isolated from a peak that eluted after the void volume of the size exclusion column, was yellow in color, and exhibited a temperature-dependent EPR signal, so it appeared that an aerobic purification at 4 °C was sufficient for isolating the holoenzyme (Figure S5). This sensitivity to O_2 could have easily been overlooked, but in the process of working with aerobically purified UvrC, we noticed that the protein bleached over the course of experiments. During a straightforward time course monitoring the absorbance band centered at 410 nm, near-complete disappearance of the signal occurred after incubating at 37 °C after 1 h, which is a common incubation temperature and time for many activity assays (Figure S5, top right).[36,98,101–103] Furthermore, most activity assays use low concentrations of enzyme such that the cofactor absorbance (and therefore integrity) is not generally monitored.

Comparison of the UV–vis spectra of aerobically purified and anaerobically purified UvrC further highlights the elusive nature of holo-UvrC. Briefly, the UV–vis absorption spectra of both proteins are similar, though there is a small feature in the UV–vis spectrum of aerobically purified UvrC at 325 nm, which could be due to the partially degraded cluster in the $[3Fe4S]^+$ state (Figure S5).[69] Differences are also seen with the chromatograms of the size exclusion column (Figure S5). Aggregated protein and what we thought was soluble protein were not as easily separated under aerobic conditions, and the soluble protein displayed an earlier elution volume. Based on the chromatogram, the yield of aerobically isolated UvrC was also lower in comparison to anaerobically isolated UvrC. We also note that postpurification, concentration steps were done aerobically at 4 °C during initial studies, so it is likely that oligomeric species were generated *in situ* prior to freezing and storing. These observations from early studies with UvrC highlight the necessity of handling this protein in an anaerobic environment to minimize heterogeneity.

Mutation of Coordinating Cysteines Leads to Instability.

To explore the site of coordination, we generated Cys → Ala mutations of the cysteine residues that are highly conserved at positions Cys154, Cys166, Cys174, and Cys178. Using the conditions optimized for overexpression, we found the Cys154Ala (Cys154 → Ala154) and Cys166Ala mutants overexpress similarly to WT UvrC (Figure S6). In contrast, expression of the Cys174Ala and Cys178Ala mutants were not detectable in whole cell lysate. The Cys154Ala and Cys166Ala mutants precipitated or aggregated, eluting at the void volume of the size exclusion column (data not shown). Attempts were made to isolate any amount of the Cys174Ala and Cys178Ala mutants, but none could be harvested (data not shown). The coordinating cysteine residues of repair and replication proteins have been found to be involved in regulating protein expression, protein stability, subunit assembly, and enzymatic activity.[64,79,104,105] The extent to which each protein, including homologous protein, is disrupted by cysteine mutations (relative to WT) appears to vary widely depending on which residue is mutated and what mutation is chosen. Overall, our observations support the assignment of Cys154, Cys166, Cys174, and Cys178 as cluster-

stabilizing residues, and examination of other regulatory aspects of the cysteines ligating the [4Fe4S] cluster of UvrC warrants further investigation.

UvrC Independently Forms a Complex with DNA Substrates.

To continue characterizing UvrC in holo form, we examined how UvrC interacts with radiolabeled, duplexed 30 base pair substrates using electrophoretic mobility shift assays (EMSAs) completed in an anaerobic chamber.[78,80,106,107] UvrC along with the full UvrABC exinuclease has been studied extensively *in vitro* with single-stranded DNA (ssDNA), well-matched (WM) double-stranded DNA (dsDNA), damaged duplex substrates, and substrates with nicks, gaps, bubbled regions, and overhangs derived from plasmid DNA and synthetic oligomers.[33,34] The majority of previous work from chromatographic, optical, and gel-based methods with UvrC from *E. coli* and thermophilic bacteria indicates that UvrC does not form a complex with dsDNA independently of UvrA and UvrB.[108–112] (It should be noted that UvrC, both truncated and full-length, has been seen to bind to ssDNA or single-stranded regions of nicked, gapped, or bubbled substrates.[37,103,111–113]) Thus, it is widely accepted that UvrC requires the action(s) of UvrA and UvrB in order to associate with substrates of duplex character.

There have, however, been two reports of UvrC species forming a complex with dsDNA at equilibrium (a tetramer in a gel-based assay) and nonequilibrium (single molecule assays) conditions.[114–116] It is not clear how these data can be reconciled. What is clear is that UvrC is sensitive to the conditions under which it is studied, exemplified by reports that UvrC has a tendency to form precipitates with itself, with UvrAB, and with DNA substrates.[35,117,118]

Since the majority of the genome in the cell is comprised of nondamaged dsDNA, we were interested in how UvrC in its holo form interacts with WM dsDNA. We also selected a fluorescein-modified substrate (F, Table S1), which is considered to mimic damage found in the cell caused by polycyclic aromatic hydrocarbons, natural substrates of the UvrABC system.[119] Once formation of WM and F duplexes was confirmed with annealing titrations (Figure S7), UvrC was incubated anaerobically with duplexed substrates at a high KCl concentration to avoid precipitation of UvrC (discussed above). Mixtures of UvrC and DNA did not appear cloudy, and no scattering was observed by UV–vis (see Figure S7). Free and complexed DNA was resolved on a native gel that was pre-equilibrated in degassed running buffer. Band intensities were quantified, and the fraction of complexed DNA as a function of free UvrC concentration was fit to the Hill equation. UvrC was found to form high affinity complexes with duplexed substrates, with apparent dissociation constants of 100 ± 20 nM and 80 ± 30 nM for WM and F substrates, respectively (n = 3 independent trials) (Figure 4). The complexes not only appear to be high affinity but also stable, even at the high KCl concentration used; band smearing was not observed over all three trials.

We note that the UvrC-DNA complex displayed a much lower mobility than free duplexes. Low mobility of UvrC on native gels has been seen previously (with and without DNA substrates) and has been attributed to the positive charge of UvrC (predicted pI of about 9) in neutral buffers, which would cause migration to the positive electrode to be unfavorable.[111] Low migration has also been attributed to precipitation of protein in the gel,[116] but we do not observe precipitation in solution (Figure S7). However, Hill coefficients >1 were found

for both WM and F substrates, suggesting there is also some possibility of oligomerization upon binding to DNA. Low mobility in our system could therefore be explained through the predicted positive charge of UvrC or to formation of high molecular weight oligomers of UvrC on DNA. In any case, we conclude that holo-UvrC forms a high affinity complex with undamaged and damaged duplexed DNA.

DNA Binding Does Not Lead to Independent Enzymatic Activity.

Our observation that holo-UvrC forms complexes with dsDNA independently of other NER proteins led us to investigate if holo-UvrC also exhibited independent or nonspecific enzymatic activity, which has been observed previously.[120,121] UvrC uniquely contains two, independent active sites, a GIY-YIG motif in the N-terminal domain which is responsible for making the incision 3′ to the site of damage and a second active site which is a structurally conserved RNase H-like domain in the C-terminal end of the protein that achieves incision 5′ to the damage site.[33] The 5′ and 3′ incisions can even be reconstituted *in vitro* with C-terminal and N-terminal truncation products of UvrC, respectively, which both exclude the Cys-rich region.

Standard activity assay conditions include Mg^{2+}, ATP, DTT (or another common reducing agent), and a KCl concentration of 0.1 M.[36,101–103,122] We first verified that buffer-exchanging UvrC into a lower-salt buffer did not cause immediate destabilization of the protein. The UV–vis spectrum indicated that [4Fe4S] cofactor was not lost in the process of buffer exchanging (Figure S7). Furthermore, size exclusion chromatography confirmed that UvrC in buffer containing 0.1 M KCl eluted at the same volume as UvrC in buffer containing 0.5 M KCl, confirming that the oligomeric state was unchanged during buffer exchange (Figure S7). We also verified that UvrC exhibited a similar binding profile to dsDNA (both WM and F substrates) in buffer that contained 0.1 M KCl as in buffer containing 0.5 M KCl (Figure S7 and see Figure 3 for comparison).

We tested the activity of UvrC at multiple concentrations on the F substrate as well as the WM substrate as a control. Even up to a concentration of 1 μM UvrC by cluster (3:1 DNA:UvrC ratio), no evidence of substrate incision by UvrC under the conditions tested was observed (Figure 5 and Figure S7). The absence of enzymatic activity in the presence of DNA binding suggests that a complicated set of factors controls UvrC activity, which appear to prevent spurious reactions from occurring even as UvrC is bound to dsDNA in holo form. How the [4Fe4S] cofactor is involved in such regulation remains to be determined. For other repair and replication proteins, the finely tuned roles of the [4Fe4S] cofactor have been examined over many studies. These studies have been particularly informative for understanding how disruption of the [4Fe4S] cofactor inhibits subunit assembly (and therefore enzymatic activity) *or* enzymatic activity alone of the multisubunit B family replication enzymes, polymerases ε and δ, respectively.[64,105,123] In the context of the multisubunit exinuclease repair complex formed by UvrABC, we speculate that because the [4Fe4S] domain is adjacent to the UvrBC interacting domain (see Figure 1), the [4Fe4S] cluster may analogously be involved in the association of UvrC with other NER proteins or the overall activity of the exinuclease complex.[7] Other roles may also exist for the [4Fe4S]

cluster of UvrC relevant for other repair pathways, one of which is possible to study because of the independent DNA binding activity of UvrC (*vide infra*).

UvrC Participates in DNA-Mediated Charge Transport (DNA CT) Chemistry.

Iron sulfur clusters are well-known electron carriers in the cell, and efforts to understand the role of electron transfer reactions in DNA repair and replication have only recently begun.[12] Using several complementary techniques, we have investigated the redox chemistry of glycosylases, SF2 $5' \rightarrow 3'$ helicases, primase, and B family replication polymerases that are found in Bacteria, Archaea, and Eukarya.[12] All proteins studied to date have been observed to access the $[4Fe4S]^{3+/2+}$ couple with midpoint potentials of ~200 mV vs NHE.[12] Binding to DNA polyanions has been shown to tune their midpoint potentials to ~80 mV vs NHE which activates the cluster toward oxidation and would allow these proteins to exchange electrons through long-range signaling through DNA as a first step in lesion detection.[12,13,124,125] A reversible signal occurs at 80 mV vs NHE, indicating that the electron transfer is not damaging for the DNA substrate or the cluster at physiological potentials. Critically, the studies of the redox activity on DNA-modified gold electrodes and other complementary-gel-based methods have demonstrated that the [4Fe4S] cluster of repair and replication enzymes can participate in DNA CT chemistry, the transport of charge through the π stack of the duplex. The efficiency of the charge transport is extraordinarily sensitive to disruption of the base stack, a common feature of damaged DNA sites.[126] We have developed models to describe how redox signaling among repair and replication proteins utilize DNA CT chemistry to facilitate repair of damage and faithful replication of the genome on a biologically relevant time scale.[12]

One of the first methods we use to interrogate the DNA-bound redox activity of a [4Fe4S] protein is electrochemistry on DNA-modified gold electrodes.[127] We have previously developed a gold electrode platform that can be modified with DNA monolayers which are formed through a thiol–gold bond on surfaces that are accessible to proteins in solution. Generally, the gold electrode serves as the working electrode, while a Ag/AgCl gel tip and a platinum wire serve as the reference electrode and auxiliary electrodes, respectively. The latest generation of DNA-modified gold electrodes features a multiplex chip with 16 independently addressable electrodes that can be separated into quadrants which allows for up to four different experimental conditions to be assayed in parallel (Figure 6). The platform has also been adapted for studies that require anaerobic conditions.[12]

Application of UvrC to DNA monolayers on a multiplex chip in buffered solution allowed for observation of a reversible, redox signal centered at a midpoint potential of 90 mV vs NHE, consistent with the redox activity observed by EPR (Figure 6). The signal increased with time, suggesting that UvrC is a diffusive species at the monolayer.[56] Varying scan rate and quantifying the anodic and cathodic peak currents in a Randles–Sevcik analysis confirmed that the redox-active species on the electrode is indeed diffusive.[74] Thus, we conclude that UvrC behaves like the other HiPIP-like repair and replication proteins we have studied that contain a [4Fe4S] cluster. Like these proteins, UvrC participates in DNA charge transport chemistry. UvrC is the fourth repair protein from *E. coli* and the sixth protein from Bacteria reported to do so.[124] Moreover, UvrC shares a DNA-bound redox potential with

EndoIII, MutY, and DinG, the three other repair proteins from *E. coli* that are known to coordinate the [4Fe4S] cofactor. Redox signaling between UvrC and DinG *in vivo* has already been suggested by the increased UV sensitivity in DinG overexpression and Δ*dinG* strains of *E. coli*. *In vivo* data suggest that redox signaling among BER, Loop Repair, and NER may be involved in facilitating growth recovery after challenge of cells with UV-light.[100,128]

Implications for UvrC as a [4Fe4S] Protein.

The data presented herein have demonstrated that UvrC coordinates a [4Fe4S] cluster that contributes to protein stability, undergoes oxidative degradation, facilitates substrate binding, and participates in DNA CT. With the discovery that UvrC is a [4Fe4S] enzyme, excision nucleases join the growing body of diverse repair and replication proteins known to bear the [4Fe4S] center. Excision nucleases are a small class of proteins, comprised of UvrC and a smaller protein Cho (UvrC homologue), found only in Bacteria and some Archaea. We predict that Cho, which is homologous to the N-terminal half of UvrC and contains the four conserved cysteine residues, may also coordinate a [4Fe4S] cluster.[129,130] Other [4Fe4S] proteins may be identified once structural data becomes available for excision nucleases. We also note that even though substrate processing by prokaryotic and eukaryotic NER machinery is similar, the proteins in each pathway that accomplish the repair are divergent. Even so, a [4Fe4S] protein has now been found in each system, UvrC and XPD (a SF2 5′ → 3′ helicase) in prokaryotic and eukaryotic NER, respectively. In a small set of archaeal species, both UvrC and XPD are encoded in the genome.[131]

Continued study of UvrC both *in vitro* and *in vivo* will help further our understanding of the relationship between UvrC activity and its [4Fe4S] cofactor (Figure 7). In the cell, [FeS] cofactors are loaded by biogenesis machinery to recipient proteins in a series of regulated and controlled steps; thus, there is a putative relationship between pathways that include UvrC (and perhaps Cho) and iron–sulfur metabolism.[7,10,20] UvrC is part of NER, in both the global genomic and the transcription-coupled subpathways, and the nature of interactions between NER proteins with newly synthesized apo-UvrC and loaded holo-UvrC remains to be examined. Recognition of structurally and chemically diverse lesions and the activity of protein complexes with apo and holo-UvrC on substrates also requires further examination. It is possible that the different forms of UvrC in the cell, apo, holo, and aggregated, may have different roles and are recognized differently by cellular components.

In its holo form, we expect that UvrC alone would be found in complex with DNA due the high affinity of the complex observed here. When bound to DNA, UvrC can participate in a redox signaling network through DNA CT chemistry, which would serve as a means for crosstalk among repair pathways *in vivo*, allowing for rapid scanning of the genome for lesions.[12,13,124,125] This study certainly highlights how the enigmatic functions of UvrC, which have eluded understanding for many years, may be related to the [4Fe4S] cofactor. We expect that future studies which carefully monitor the [4Fe4S] cofactor will continue to unravel key aspects regarding the activity of UvrC *in vitro* and *in vivo*.

EXPERIMENTAL SECTION

General Procedures.

All reagents were used as received and stored according the manufacturer's instructions. All water used was purified on a Milli-Q Reference Ultrapure Water Purification System (≥18.2 MΩ cm). Anaerobic vinyl chambers (glove bags) were kept at atmospheres of (2–4% H_2 in Argon or N_2, ≤1 ppm of O_2) with Pd scrubbing towers (Coy Laboratories) and used for experiments requiring anaerobic conditions. Unless specified otherwise, all protein buffers were degassed in an anaerobic chamber by stirring vigorously overnight. Protein samples were handled anaerobically, and other solutions of reagents that came in contact with UvrC were prepared anaerobically as well.[132–134] UV–vis spectra of UvrC were taken on a Cary 100 Bio (Agilent) spectrophotometer using custom quartz cuvettes (Starna) modified with an airtight screwcap or on a DeNovix DS-C Spectrophotometer using quartz cuvettes (Starna) in the glovebag. DNA concentrations were taken as above aerobically. High performance liquid chromatography (HPLC) was done using an HP 1100 (Aglient) system, and fast performance liquid chromatography (FPLC) was done using an ÄKTA FPLC system (GE Life Sciences) or a NGC Chromatography System (Bio-Rad). Before use, all solvents and buffers used during purifications were filtered through a 0.22 or 0.45 μm Nalgene Rapid-Flow filter unit with an SFCA membrane (ThermoFisher Scientific). Glass plates, spacers, and the Owl Vertical Electrophoresis System were purchased from ThermoFisher Scientific. Sequencing gel supplies were purchased from National Diagnostics.

Multiple Sequence Alignments.

UvrC sequences from *Escherichia coli* (*E. coli*), *Salmonella typhimurium* (*S. typhimurium*), *Pseudomonas aeruginosa* (*P. aeruginosa*), *Staphylococcus aureus* (*S. aureus*), *Mycobacterium tuberculosis* (*M. tuberculosis*), *Thermotoga maritima* (*T. maritima*), and *Methanosarcina acetivorans* (*M. acetivorans*) were aligned using TCoffee (tcoffee.crg.org), and alignments were formatted using BoxShade (ExPasy). Sequences were placed in decreasing order of taxonomic relationship.

Overexpression of UvrC.

A starter culture of One Shot TOP10 Electrocomp *E. coli* Cells (Invitrogen) containing the UvrC overexpression plasmid (encoding the His_6-MBP-UvrC fusion protein) or Cys→Ala mutant overexpression plasmids were grown (200 rpm, 37 °C) ~16 h in LB/Amp (50 mg/L). Large (1 L) cultures LB/Amp (50 mg/L) were inoculated with starter culture and grown (225 rpm, 37 °C) to an OD_{600} of ~0.6, and expression was induced by addition of arabinose to a final concentration of 10 mg/L. Cells were grown for 16 h (150 rpm, 22 °C), harvested at 5000 rpm for 20 min, and stored at −80 °C.

Degassing Purification Buffers.

The following purification buffers were prepared at a pH of 7.5: Lysis Buffer (25 mM Tris-HCl, 0.5 M KCl, 10% v/v glycerol), Nickel Elution Buffer (25 mM Tris-HCl, 0.5 M KCl, 20% v/v glycerol, 0.5 M Imidazole), and Size Exclusion Buffer (25 mM Tris-HCl, 0.5 M KCl, 20% v/v glycerol). The buffers were placed in separate round-bottom flasks with

custom glass adapters, connected to a Schlenk line, and degassed using a timer (Eagle Signal) alternating vacuum (7 min) and Ar (2 min) for 12 cycles.[66,67]

Anaerobic Purification of UvrC and Cys→Ala Mutants.

Described is the procedure for purifying UvrC that was adapted from the purification method for nitrogenase;[66,67] the procedure is identical for Cys→Ala mutants. Two, stacked HisTrap HP 5 mL columns (GE Healthcare) and a Superdex 200 preparative grade 26/200 size exclusion column (GE Healthcare) were used for purification. Nickel columns were washed with at least 5 column volumes (10 mL, ColVs) of ddH_2O, and the Superdex column was washed with 1.5 to 2 ColVs of ddH_2O. Once buffers were degassed, the Superdex 200 was washed with 1.5 to 2 ColV (330 mL) of size exclusion buffer overnight. The next day, the Superdex 200 was equilibrated with an additional 100 mL of degassed size exclusion buffer containing 1 mM DTT. The HisTrap columns were washed with >10 ColV of lysis buffer with 1 mM DTT. The day of purification, DTT was also added to elution buffer to a final concentration of 1 mM. All following steps were completed in an anaerobic chamber, on a Schlenk line, or in airtight vials. While columns were equilibrating, cell pellets were thawed, resuspended in Lysis Buffer (100 mL lysis buffer per 10 g of wet pellet) that was supplemented on the day of the purification with 6–8 tablets of crushed cOmplete protease inhibitor cocktail tablets (Roche), DNase (15 kU, Sigma), and DTT (1 mM), and homogenized on ice using a Dounce homogenizer. The cell slurry was passed over a 100 μm nylon cell strainer (Corning) and lysed using an Emulsiflex-C5 (Avestin) homogenizer at 25 000 psi under a positive pressure of Ar over two cycles. For each cycle, cell lysate was collected on ice. Lysate was loaded into polycarbonate vials and centrifuged on a Sorvall RC 6 Plus Centrifuge (ThermoFisher-Scientific) at 13 000 rpm for 45 min at 4 °C.

Using an ÄKTA FPLC system (GE Life Sciences), the supernatant was loaded under a positive pressure of Ar at a flow rate of 2.5 mL/min onto the HisTrap column. At a flow rate of 1.5 mL/min, Histrap columns were washed with 4 ColVs of 10% Elution Buffer and eluted with 10 to 100% Elution Buffer over 15 ColVs. Fractions were collected under a positive pressure of Ar and concentrated to <10 mL using an Amicon Stirred Ultrafiltration Cell over a 30 kDa cutoff filter using the minimum overpressure that allowed for filtration. Concentrated fractions were loaded under a positive pressure of Ar onto the Superdex 200 at a flow rate of 1 mL/min. Samples were eluted with 1 ColV of Size Exclusion Buffer containing 1 mM DTT. Soluble fractions were collected, concentrated between 20 and 30 μM to avoid precipitation upon freezing, aliquoted in screw cap vials, then immediately flash frozen in liquid N_2, and stored at ≤ −80 °C. Subfractions were taken throughout the purification to assess the purity of the samples by SDS-PAGE as above, combining Blue Loading Buffer (NEB) 1:1 with fractions, preheating in sample buffer at 80 °C for 2 min before resolving on a 4–20% TGX precast gel (Bio-Rad) at 200 V for 35 min.

UV–Vis and Continuous Wave (CW) Electron Paramagnetic Resonance (EPR) Spectroscopies.

For all assays described below, aliquots of UvrC were thawed on ice in an anaerobic chamber and buffer-exchanged by diafiltration into UvrC buffer (25 mM Tris-HCl, 0.5 M KCl, 20% v/v glycerol) using Amicon Ultra-0.5 mL 10 kDa cut off mini filter units

(Millipore). The [4Fe4S] cluster concentration was quantified by using the extinction coefficient of the absorption band centered at 410 nm (ε = of 17 000 $M^{-1}\cdot cm^{-1}$).[59] Because of the size of the fusion protein, typically a 10–15× dilution of the thawed protein needed to be made in order bring the absorption band at 280 nm into the linear region. The total protein concentration was then quantified by using the calculated excitation coefficient (Expasy) of His_6-MBP-UvrC at 280 nm (ε = 111 995 $M^{-1}\cdot cm^{-1}$). The percent of the [4Fe4S] cofactor incorporated was calculated by dividing the total concentration of [4Fe4S] over the total protein concentration. EPR samples were prepared in 200 μL volumes at final concentrations of UvrC at 10 μM and ferricyanide at 50 μM in UvrC buffer. Samples were loaded into clean 4 mm thin-wall precision quartz EPR tubes (Wilmad LabGlass, 715-PW-250MM), capped, and flash frozen in liquid N_2. An EMX X-band spectrometer (Bruker) with an ESR-900 cryogen flow cryostat (Oxford) and an ITC-503 temperature controller was used to collect X-band CW EPR spectra. Spectra were acquired at 10 K at power settings between 12 and 16 mW and a modulation amplitude of 10 gauss using WinEPR software (Bruker).[80] Data presented were collected in triplicate.

Fe Quantification by the Ferene Assay.

The colorimetric ferene assay was performed according to a published procedure in triplicate.[80] Briefly, samples (including a UvrC buffer control) were diluted 1:1 with HNO_3 (21.7% v/v) to a total volume of 200 μL. Samples were heated at 95 °C for 30 min, cooled at 4 °C for at least 10 min, and centrifuged. After centrifugation, 600 μL of ammonium acetate (7.5% w/v), 100 μL of ascorbic acid (12.5% w/v), and 100 μL of 3-(2-pyridyl)-5,6-di(2-furyl)-1,2,4-triazine-5′,5″-disulfonate (ferene, 10 mM) were added. Samples were incubated at room temperature for 30 min before absorbance at 593 nm was recorded. Calibration curves were prepared using an Fe standard solution (1001 ± 2 mg/L Fe in 2% v/v HNO_3, TraceCERT Fe standard for ICP).

Assessment of UvrC Stability.

To investigate the stability of UvrC under aerobic conditions, UvrC was thawed on ice in a cold room and then buffer exchanged into aerobic UvrC buffer as described above. UvrC was quantified by UV–vis as above in Starna cuvettes that were sealed with a screw cap (to prevent evaporation) before heating in a 37 °C water bath. Generally, between 10 μM and 30 μM of UvrC (by cluster) was used. For each time point, the Cary instrument was blanked with buffer at 37 °C. Samples at a concentration of 5 μM were loaded into a Hamilton syringe, injected into a 250 μL superloop on a Bio-Rad NGC, and applied to a Superdex 100/300L analytical size exclusion column (GE Healthcare) at a flow rate of 0.35 mL/min in UvrC buffer. An aliquot of protein was reserved and analyzed by SDS-PAGE as above. Samples that included DNA substrates were treated as above, and WM duplexes were added 1:1 with holo-UvrC (ex. 20 μM DNA and 20 μM UvrC by cluster). UvrC samples that included WM dsDNA were measured against buffer that included the same concentration of DNA. For comparison, UvrC was also heated anaerobically in UvrC buffer in a capped microfuge tube on a heat block in the glovebag and assessed as above. UvrC was also buffer exchanged anaerobically into 25 mM Tris-HCl, 0.1 M KCl, and 20% glycerol (v/v) at a pH of 7.5 (activity buffer) and examined by size exclusion chromatography as above. UvrC in low-salt activity buffer was used immediately in downstream assays.

Electrophoretic Mobility Shift Assays (EMSA).[78,80,106,107]

Native PAGE running buffer (25 mM Tris, 192 mM glycine, pH 8.3 from Bio-Rad) was degassed overnight in an anaerobic chamber with vigorous stirring. The duplex character of substrates was assessed by an annealing titration (see Supporting Experimental Section), and completely annealed duplexes were used for EMSAs and in activity assays (see below). Radioactivity was detected using an LS 6000SC Scintillation Counter (Beckman). In an anaerobic chamber, 10 nM to 2 μM UvrC (by cluster) was incubated for 30 min at room temperature with 100 nM dsDNA in activity buffer or UvrC buffer. DNA protein mixtures were electrophoresed at 50 V for 2 h at room temperature using Mini-PROTEAN TGX 4–20% Precast Gels (Bio-Rad). Gels were exposed on a phosporimaging screen as described in the Supporting Experimental Section. For each replicate, bands were quantified using Image Lab (Bio-Rad) and the fraction of bound DNA was plotted as a function of free UvrC concentration and fit to the Hill function using Origin (OriginLab Corporation). The apparent dissociation constant reported is the free UvrC concentration when half of the DNA substrates are bound. From three independent trials, the apparent dissociation constants were averaged over and are reported with the standard error of the mean.

Incision Assays.[36,102,103,106,107,113,116,119,122,135]

In an anaerobic chamber, UvrC was buffer exchanged into activity buffer. Solutions of $MgCl_2$, ATP, and DTT were prepared in the glovebag in filtered and degassed water (Trials 1 and 2) or in filtered and degassed buffer containing 25 mM Tris-HCl, 0.1 M KCl, and 20% v/v glycerol. UvrC was preincubated at room temperature with 10 mM $MgCl_2$ and 1 mM DTT. Just before addition of 3 μM ^{32}P-dsDNA (WM or F), 10 mM ATP was added to UvrC and samples were incubated at 37 °C for 1 h and then heat inactivated at 70 °C for >10 min. Radioactivity was quantified using the Beckman LS 6000SC Scintillation Counter (Beckman). Samples were mixed 1:1 with denaturing loading dye (80% formamide, 10 mM sodium hydroxide, 0.025% xylene cyanol, and 0.025% bromophenol blue, in TBE buffer from National Diagnostics [0.089 M Tris base, 0.089 M boric acid, and 2 mM Na_2EDTA at pH 8.3]) and stored at −20 °C until use. A 20% TBE-Urea polyacrylamide sequencing gel was preheated to over 50 °C, and then samples were resolved on the preheated gel for 120 min at 90 W. Gels were exposed on a phosporimaging screen, imaged, and visualized as described.

DNA-Modified Electrochemistry on Au Surfaces.[59,127,136]

A 16-electrode, gold, multiplex chip (4 quadrants with 4 electrodes each) was rinsed and sonicated with acetone three times for 5 min and once with 100% isopropyl alcohol, also for 5 min. The gasket and clamp were washed and sonicated in 50% isopropanol (in water) for 5 min followed by three to five rinses with water. All components were dried using an argon gun. To clear the chip of debris, the chip was cleaned by ozonolysis (UVO Cleaner) for 15 min. The chip, gasket, and clamp were assembled and 23 μL duplexed WM electrochemistry substrate at a concentration of 25 μM (see Supporting Experimental Section) were added to each quadrant. Monolayers were allowed to form overnight under humid conditions at room temperature. The electrode was then rinsed three times with DNA buffer (5 mM sodium phosphate, 50 mM NaCl, pH 7.0) and then three times with glycerol buffer (DNA buffer

with 5% glycerol). The electrode was backfilled with 1 mM of 6-mercaptohexanol (in glycerol buffer) for ~30 min. The electrode was rinsed 10 times with DNA buffer. In an anaerobic chamber, 400 μL of 5 μM of UvrC (by cluster) were added to the chip in electrochemistry buffer (4 mM spermidine, 25 mM Tris-HCl, pH 7.5, 0.25 M KCl, 20% glycerol). A 4% agarose/3 M NaCl gel tip Ag/AgCl reference electrode (MW-2030, RE-6, BASi) was used. The potentiostat, multiplexer, and analysis software were from CH Instruments, Inc. A scan rate of 50–100 mV/s between −0.4 and 0.2 V (vs Ag/AgCl) is optimal for cyclic voltammograms. Scans were taken periodically at 0, 1, 2, and 3 h. Square wave scans were taken after 3 h, and then scan rates were varied from 10 to 1600 mV/s. A Randles–Sevcik analysis was done by plotting the current vs scan rate and $(\text{scan rate})^{1/2}$. Data presented are representative of three independent trials.

Supplementary Material

Refer to Web version on PubMed Central for supplementary material.

ACKNOWLEDGMENTS

We are grateful to the NIH (RM35GM126904 to J.K.B.) and The Gordon and Betty Moore Foundation (to the Caltech Center for the Chemistry of Cellular Signaling) for their financial support. R.M.B.S. recognizes the National Science Foundation (NSF) for support through a Graduate Research Fellowship and the Center for Environmental Microbial Interactions (CEMI, Caltech) through a Pilot Grant. M.A.G. was an NIH predoctoral trainee (NIH/NRSA 5T32GM07616) and also a recipient of a CEMI Pilot Grant. The authors are especially grateful to the Rees group at Caltech, particularly Ailiena Maggiolo, for use of their vacuum manifold for anaerobic purification of UvrC. The authors also thank undergraduate researchers, Jenny He and Sirus Han, who contributed to early studies with cysteine mutants. This work was also facilitated by use of the Caltech EPR facility which is supported by the NSF (NSF-1531940) and the Dow Next Generation Educator Fund. In addition, we thank A. Boal for her early insights regarding UvrC and a possible association with a [4Fe4S] cluster.

REFERENCES

(1). Beinert H; Holm RH; Münck E Iron-Sulfur Clusters: Nature’s Modular, Multipurpose Structures. Science 1997, 277 (5326), 653–659. [PubMed: 9235882]

(2). Rees DC; Howard JB The Interface between the Biological and Inorganic Worlds: Iron-Sulfur Metalloclusters. Science 2003, 300 (5621), 929–931. [PubMed: 12738849]

(3). Sweeney WV; Rabinowitz JC Proteins Containing 4Fe-4S Clusters: An Overview. Annu. Rev. Biochem 1980, 49 (1), 139–161. [PubMed: 6250442]

(4). Fontecave M Iron-Sulfur Clusters: Ever-Expanding Roles. Nat. Chem. Biol 2006, 2 (4), 171–174. [PubMed: 16547473]

(5). Liu J; Chakraborty S; Hosseinzadeh P; Yu Y; Tian S; Petrik I; Bhagi A; Lu Y Metalloproteins Containing Cytochrome, Iron-Sulfur, or Copper Redox Centers. Chem. Rev 2014, 114 (8), 4366–4369. [PubMed: 24758379]

(6). Mettert EL; Kiley PJ Fe-S Proteins That Regulate Gene Expression. Biochim. Biophys. Acta, Mol. Cell Res 2015, 1853 (6), 1284–1293.

(7). Fuss JO; Tsai CL; Ishida JP; Tainer JA Emerging Critical Roles of Fe-S Clusters in DNA Replication and Repair. Biochim. Biophys. Acta, Mol. Cell Res 2015, 1853 (6), 1253–1271.

(8). White MF; Dillingham MS Iron-Sulphur Clusters in Nucleic Acid Processing Enzymes. Curr. Opin. Struct. Biol 2012, 22 (1), 94–100. [PubMed: 22169085]

(9). Andreini C; Banci L; Rosato A Exploiting Bacterial Operons to Illuminate Human Iron-Sulfur Proteins. J. Proteome Res 2016, 15 (4), 1308–1322. [PubMed: 26889782]

(10). Puig S; Ramos-Alonso L; Romero AM; Martínez-Pastor MT The Elemental Role of Iron in DNA Synthesis and Repair. Metallomics 2017, 9 (11), 1483–1500. [PubMed: 28879348]

(11). Lessner FH; Jennings ME; Hirata A; Duin EC; Lessner DJ Subunit D of RNA Polymerase from Methanosarcina Acetivorans Contains Two Oxygen-Labile [4Fe-4S] Clusters: Implications for Oxidant-Dependent Regulation of Transcription. J. Biol. Chem 2012, 287 (22), 18510–18523. [PubMed: 22457356]

(12). Barton JK; Silva RMB; O'Brien E Redox Chemistry in the Genome: Emergence of the [4Fe4S] Cofactor in Repair and Replication. Annu. Rev. Biochem 2019, 88 (1), 163–190. [PubMed: 31220976]

(13). Bartels PL; O'Brien E; Barton JK DNA Signaling by Iron-Sulfur Cluster Proteins In Biochemistry, Biosynthesis and Human Diseases: Biochemistry, Biosynthesis, and Human Diseases; Rouault TA, Ed.; De Gruyter: Berlin, Boston, 2017; Vol. 2, pp 405–423. DOI:10.1515/9783110479850-015.

(14). Bartels PL; Stodola JL; Burgers PMJ; Barton JK A Redox Role for the [4Fe4S] Cluster of Yeast DNA Polymerase *δ*. J. Am. Chem. Soc 2017, 139 (50), 18339–18348. [PubMed: 29166001]

(15). O'Brien E; Holt ME; Thompson MK; Salay LE; Ehlinger AC; Chazin WJ; Barton JK The [4Fe4S] Cluster of Human DNA Primase Functions as a Redox Switch Using DNA Charge Transport. Science 2017, 355 (6327), No. eaag1789. [PubMed: 28232525]

(16). Cvetkovic A; Menon AL; Thorgersen MP; Scott JW; Poole FL; Jenney FE; Lancaster WA; Praissman JL; Shanmukh S; Vaccaro BJ; Trauger SA; Kalisiak E; Apon JV; Siuzdak G; Yannone SM; Tainer JA; Adams MWW Microbial Metalloproteomes Are Largely Uncharacterized. Nature 2010, 466 (7307), 779–782. [PubMed: 20639861]

(17). Rouault TA Iron-Sulfur Proteins Hiding in Plain Sight. Nat. Chem. Biol 2015, 11 (7), 442–445. [PubMed: 26083061]

(18). Tsai CL; Tainer JA Robust Production, Crystallization, Structure Determination, and Analysis of [Fe–S] Proteins: Uncovering Control of Electron Shuttling and Gating in the Respiratory Metabolism of Molybdopterin Guanine Dinucleotide Enzymes. Methods Enzymol. 2018, 599, 157–196. [PubMed: 29746239]

(19). Maio N; Singh A; Uhrigshardt H; Saxena N; Tong WH; Rouault TA Cochaperone Binding to LYR Motifs Confers Specificity of Iron Sulfur Cluster Delivery. Cell Metab. 2014, 19 (3), 445–457. [PubMed: 24606901]

(20). Rouault TA Mammalian Iron-Sulphur Proteins: Novel Insights into Biogenesis and Function. Nat. Rev. Mol. Cell Biol 2015, 16 (1), 45–55. [PubMed: 25425402]

(21). Zheng C; Dos Santos PC Metallocluster Transactions: Dynamic Protein Interactions Guide the Biosynthesis of Fe–S Clusters in Bacteria. Biochem. Soc. Trans 2018, 46 (6), 1593–1603. [PubMed: 30381339]

(22). Tsai-Wu JJ; Liu HF; Lu a L. Escherichia Coli MutY Protein Has Both N-Glycosylase and Apurinic/Apyrimidinic Endonuclease Activities on A.C and A.G Mispairs. Proc. Natl. Acad. Sci. U. S. A 1992, 89 (18), 8779–8783. [PubMed: 1382298]

(23). Michaels ML; Pham L; Nghiem Y; Cruz C; Miller JH MutY, an Adenine Glycosylase Active on G-A Mispairs, Has Homology to Endonuclease III. Nucleic Acids Res. 1990, 18 (13), 3841–3845. [PubMed: 2197596]

(24). Porello SL; Williams SD; Kuhn H; Michaels ML; David SS Specific Recognition of Substrate Analogs by the DNA Mismatch Repair Enzyme MutY. J. Am. Chem. Soc 1996, 118 (44), 10684–10692.

(25). Ren B; Duan X; Ding H Redox Control of the DNA Damage-Inducible Protein DinG Helicase Activity via Its Iron-Sulfur Cluster. J. Biol. Chem 2009, 284 (8), 4829. [PubMed: 19074432]

(26). Brown LT; Sutera VA; Zhou S; Weitzel CS; Cheng Y; Lovett ST Connecting Replication and Repair: YoaA, a Helicase-Related Protein, Promotes Azidothymidine Tolerance through Association with Chi, an Accessory Clamp Loader Protein. PLoS Genet. 2015, 11 (11), No. e1005651. [PubMed: 26544712]

(27). Cunningham RP; Asahara H; Bank JF; Scholes CP; Salerno JC; Surerus K; Munck E; McCracken J; Peisach J; Emptage MH Endonuclease III Is an Iron-Sulfur Protein. Biochemistry 1989, 28 (10), 4450–4455. [PubMed: 2548577]

(28). Asahara H; Wistort PM; Bank JF; Bakerian RH; Cunningham RP Purification and Characterization of Escherichia Coli Endonuclease III from the Cloned Nth Gene. Biochemistry 1989, 28 (10), 4444–4449. [PubMed: 2669955]

(29). David SS; Williams SD Chemistry of Glycosylases and Endonucleases Involved in Base-Excision Repair. Chem. Rev 1998, 98 (3), 1221–1262. [PubMed: 11848931]

(30). Wu Y; Brosh RM DNA Helicase and Helicase-Nuclease Enzymes with a Conserved Iron-Sulfur Cluster. Nucleic Acids Res. 2012, 40 (10), 4247–4260. [PubMed: 22287629]

(31). Voloshin ON; Vanevski F; Khil PP; Camerini-Otero RD Characterization of the DNA Damage-Inducible Helicase DinG from Escherichia Coli. J. Biol. Chem 2003, 278 (30), 28284–28293. [PubMed: 12748189]

(32). Reardon JT; Sancar A Purification and Characterization of Escherichia Coli and Human Nucleotide Excision Repair Enzyme Systems. Methods Enzymol. 2006, 408, 189–213. [PubMed: 16793370]

(33). Kisker C; Kuper J; Van Houten B. Van; Van Houten B Prokaryotic Nucleotide Excision Repair. Cold Spring Harbor Perspect. Biol 2013, 5 (3), a012591.

(34). Truglio JJ; Croteau DL; van Houten B; Kisker C Prokaryotic Nucleotide Excision Repair: The UvrABC System. Chem. Rev 2006, 106 (2), 233–252. [PubMed: 16464004]

(35). Thomas DC; Levy M; Sancar A Amplification and Purification of UvrA, UvrB, and UvrC Proteins of Escherichia Coli. J. Biol. Chem 1985, 260 (17), 9875–9883. [PubMed: 2991268]

(36). Sancar A; Rupp WD A Novel Repair Enzyme: UVRABC Excision Nuclease of Escherichia Coli Cuts a DNA Strand on Both Sides of the Damaged Region. Cell 1983, 33 (1), 249–260. [PubMed: 6380755]

(37). Sancar A; Kacinski BM; Mott DL; Rupp WD Identification of the UvrC Gene Product. Proc. Natl. Acad. Sci. U. S. A 1981, 78 (9), 5450–5454. [PubMed: 7029536]

(38). Yoakum GH; Grossman L Identification of E. Coli UvrC Protein. Nature 1981, 292 (5819), 171–173. [PubMed: 6264323]

(39). Van Houten B Nucleotide Excision Repair in Escherichia Coli. Microbiol. Rev 1990, 54 (1), 18–51. [PubMed: 2181258]

(40). Taniguchi Y; Choi PJ; Li G-W; Chen H; Babu M; Hearn J; Emili A; Xie XS Quantifying *E. Coli* Proteome and Transcriptome with Single-Molecule Sensitivity in Single Cells. Science 2010, 329 (5991), 533–538. [PubMed: 20671182]

(41). Li G-W; Burkhardt D; Gross C; Weissman JS Quantifying Absolute Protein Synthesis Rates Reveals Principles Underlying Allocation of Cellular Resources. Cell 2014, 157 (3), 624–635. [PubMed: 24766808]

(42). Imlay JA The Molecular Mechanisms Andphysiological Consequences of Oxidativestress: Lessons from a Model Bacterium. Nat. Rev. Microbiol 2013, 11 (7), 443–454. [PubMed: 23712352]

(43). Kuzminov A Recombinational Repair of DNA Damage in Escherichia Coli and Bacteriophage Lambda. Microbiol. Mol. Biol. Rev 1999, 63 (4), 751–813. [PubMed: 10585965]

(44). Kapust RB; Waugh DS Escherichia Coli Maltose-Binding Protein Is Uncommonly Effective at Promoting the Solubility of Polypeptides to Which It Is Fused. Protein Sci. 1999, 8 (8), 1668–1674. [PubMed: 10452611]

(45). Baneyx F Recombinant Protein Expression in Escherichia Coli. Curr. Opin. Biotechnol 1999, 10 (5), 411–421. [PubMed: 10508629]

(46). Kapust RB; Tözsér J; Fox JD; Anderson DE; Cherry S; Copeland TD; Waugh DS Tobacco Etch Virus Protease: Mechanism of Autolysis and Rational Design of Stable Mutants with Wild-Type Catalytic Proficiency. Protein Eng. 2001, 14 (12), 993–1000. [PubMed: 11809930]

(47). Sun P; Tropea JE; Waugh DS Enhancing the Solubility of Recombinant Proteins in Escherichia Coli by Using Hexahistidine-Tagged Maltose-Binding Protein as a Fusion Partner. Methods Mol. Biol 2011, 705, 259–274. [PubMed: 21125392]

(48). Guzman LM; Belin D; Carson MJ; Beckwith J Tight Regulation, Modulation, and High-Level Expression by Vectors Containing the Arabinose P(BAD) Promoter. J. Bacteriol 1995, 177 (14), 4121–4130. [PubMed: 7608087]

(49). Rosano GL; Ceccarelli EA Recombinant Protein Expression in Escherichia Coli: Advances and Challenges. Front. Microbiol 2014, 5 (APR). DOI: 10.3389/fmicb.2014.00172.

(50). Sørensen HP; Mortensen KK Advanced Genetic Strategies for Recombinant Protein Expression in Escherichia Coli. J. Biotechnol 2005, 115 (2), 113–128. [PubMed: 15607230]

(51). Terpe K Overview of Bacterial Expression Systems for Heterologous Protein Production: From Molecular and Biochemical Fundamentals to Commercial Systems. Appl. Microbiol. Biotechnol 2006, 72 (2), 211–222. [PubMed: 16791589]

(52). Shimberg GD; Pritts JD; Michel SLJ Iron–Sulfur Clusters in Zinc Finger Proteins. Methods Enzymol. 2018, 599, 101–137. [PubMed: 29746237]

(53). Klinge S; Hirst J; Maman JD; Krude T; Pellegrini L An Iron-Sulfur Domain of the Eukaryotic Primase Is Essential for RNA Primer Synthesis. Nat. Struct. Mol. Biol 2007, 14 (9), 875–877. [PubMed: 17704817]

(54). Boal AK; Yavin E; Lukianova OA; O'Shea VL; David SS; Barton JK DNA-Bound Redox Activity of DNA Repair Glycosylases Containing [4Fe-4S] Clusters. Biochemistry 2005, 44 (23), 8397–8407. [PubMed: 15938629]

(55). Lin JJ; Sancar A The C-Terminal Half of UvrC Protein Is Sufficient to Reconstitute (A)BC Excinuclease. Proc. Natl. Acad. Sci. U. S. A 1991, 88 (15), 6824–6828. [PubMed: 1862106]

(56). Boon EM; Livingston AL; Chmiel NH; David SS; Barton JK DNA-Mediated Charge Transport for DNA Repair. Proc. Natl. Acad. Sci. U. S. A 2003, 100 (22), 12543–12547. [PubMed: 14559969]

(57). Yavin E; Boal AK; Stemp EDA; Boon EM; Livingston AL; O'Shea VL; David SS; Barton JK Protein-DNA Charge Transport: Redox Activation of a DNA Repair Protein by Guanine Radical. Proc. Natl. Acad. Sci. U. S. A 2005, 102 (10), 3546–3551. [PubMed: 15738421]

(58). Cheng K; Wigley DB DNA Translocation Mechanism of an XPD Family Helicase. eLife 2018, 7, No. e42400. [PubMed: 30520735]

(59). Grodick MA; Segal HM; Zwang TJ; Barton JK DNA-Mediated Signaling by Proteins with 4Fe-4S Clusters Is Necessary for Genomic Integrity. J. Am. Chem. Soc 2014, 136 (17), 6470–6478. [PubMed: 24738733]

(60). Yeeles JTP; Cammack R; Dillingham MS An Iron-Sulfur Cluster Is Essential for the Binding of Broken DNA by AddAB-Type Helicase-Nucleases. J. Biol. Chem 2009, 284 (12), 7746–7755. [PubMed: 19129187]

(61). Rudolf J; Makrantoni V; Ingledew WJ; Stark MJR; White MF The DNA Repair Helicases XPD and FancJ Have Essential Iron-Sulfur Domains. Mol. Cell 2006, 23 (6), 801–808. [PubMed: 16973432]

(62). Fan L; Fuss JO; Cheng QJ; Arvai AS; Hammel M; Roberts VA; Cooper PK; Tainer JA XPD Helicase Structures and Activities: Insights into the Cancer and Aging Phenotypes from XPD Mutations. Cell 2008, 133 (5), 789–800. [PubMed: 18510924]

(63). Wolski SC; Kuper J; Hänzelmann P; Truglio JJ; Croteau DL; Van Houten B; Kisker C Crystal Structure of the FeS Cluster-Containing Nucleotide Excision Repair Helicase XPD. PLoS Biol. 2008, 6 (6), 1332–1342.

(64). Netz DJA; Stith CM; Stümpfig M; Köpf G; Vogel D; Genau HM; Stodola JL; Lill R; Burgers PMJ; Pierik AJ Eukaryotic DNA Polymerases Require an Iron-Sulfur Cluster for the Formation of Active Complexes. Nat. Chem. Biol 2012, 8 (1), 125–132.

(65). Vaithiyalingam S; Warren EM; Eichman BF; Chazin WJ Insights into Eukaryotic DNA Priming from the Structure and Functional Interactions of the 4Fe-4S Cluster Domain of Human DNA Primase. Proc. Natl. Acad. Sci. U. S. A 2010, 107 (31), 13684–13689. [PubMed: 20643958]

(66). Spatzal T; Perez KA; Einsle O; Howard JB; Rees DC Ligand Binding to the FeMo-Cofactor: Structures of CO-Bound and Reactivated Nitrogenase. Science 2014, 345 (6204), 1620–1623. [PubMed: 25258081]

(67). Wenke BB; Spatzal T; Rees DC Site-Specific Oxidation State Assignments of the Iron Atoms in the [4Fe:4S]2+/1+/0 States of the Nitrogenase Fe-Protein. Angew. Chem., Int. Ed 2019, 58 (12), 3894–3897.

(68). Gray HB; Stiefel EI; Valentine JS; Bertini I Bioinorganic Chemistry; University Books: 2006.

(69). Lippard SJ; Berg JM Principles of Bioinorganic Chemistry; University Science Books: Mill Valley, CA, 1994.

(70). Freibert SA; Weiler BD; Bill E; Pierik AJ; Mühlenhoff U; Lill R Biochemical Reconstitution and Spectroscopic Analysis of Iron–Sulfur Proteins. Methods Enzymol. 2018, 599, 197–226. [PubMed: 29746240]

(71). Chmiel NH; Golinelli MP; Francis AW; David SS Efficient Recognition of Substrates and Substrate Analogs by the Adenine Glycosylase MutY Requires the C-Terminal Domain. Nucleic Acids Res. 2001, 29, 553. [PubMed: 11139626]

(72). Messick TE; Chmiel NH; Golinelli MP; Langer MR; Joshua-Tor L; David SS Noncysteinyl Coordination to the [4Fe-4S]2+ Cluster of the DNA Repair Adenine Glycosylase MutY Introduced via Site-Directed Mutagenesis. Structural Characterization of an Unusual Histidinyl-Coordinated Cluster. Biochemistry 2002, 41 (12), 3931–3942. [PubMed: 11900536]

(73). Pokharel S; Campbell JL Cross Talk between the Nuclease and Helicase Activities of Dna2: Role of an Essential Iron-Sulfur Cluster Domain. Nucleic Acids Res. 2012, 40 (16), 7821–7830. [PubMed: 22684504]

(74). Bartels PL; Zhou A; Arnold AR; Nuñez NN; Crespilho FN; David SS; Barton JK Electrochemistry of the [4Fe4S] Cluster in Base Excision Repair Proteins: Tuning the Redox Potential with DNA. Langmuir 2017, 33 (10), 2523–2530. [PubMed: 28219007]

(75). O'Brien E; Salay LE; Epum EA; Friedman KL; Chazin WJ; Barton JK Yeast Require Redox Switching in DNA Primase. Proc. Natl. Acad. Sci. U. S. A 2018, 115 (52), 13186–13191. [PubMed: 30541886]

(76). O'Brien E; Holt ME; Salay LE; Chazin WJ; Barton JK Substrate Binding Regulates Redox Signaling in Human DNA Primase. J. Am. Chem. Soc 2018, 140 (49), 17153–17162. [PubMed: 30433774]

(77). Ha Y; Arnold AR; Nuñez NN; Bartels PL; Zhou A; David SS; Barton JK; Hedman B; Hodgson KO; Solomon EI Sulfur K-Edge XAS Studies of the Effect of DNA Binding on the [Fe4S4] Site in EndoIII and MutY. J. Am. Chem. Soc 2017, 139 (33), 11434–11442. [PubMed: 28715891]

(78). Tse ECM; Zwang TJ; Barton JK The Oxidation State of [4Fe4S] Clusters Modulates the DNA-Binding Affinity of DNA Repair Proteins. J. Am. Chem. Soc 2017, 139 (36), 12784–12792. [PubMed: 28817778]

(79). McDonnell KJ; Chemler JA; Bartels PL; O'Brien E; Marvin ML; Ortega J; Stern RH; Raskin L; Li GM; Sherman DH; Barton JK; Gruber SB A Human MUTYH Variant Linking Colonic Polyposis to Redox Degradation of the [4Fe4S]2+cluster. Nat. Chem 2018, 10 (8), 873–880. [PubMed: 29915346]

(80). Ekanger LA; Oyala PH; Moradian A; Sweredoski MJ; Barton JK Nitric Oxide Modulates Endonuclease III Redox Activity by a 800 MV Negative Shift upon [Fe4S4] Cluster Nitrosylation. J. Am. Chem. Soc 2018, 140 (37), 11800–11810. [PubMed: 30145881]

(81). Thayer MM; Ahern H; Xing D; Cunningham RP; Tainer JA Novel DNA Binding Motifs in the DNA Repair Enzyme Endonuclease III Crystal Structure. EMBO J. 1995, 14, 4108. [PubMed: 7664751]

(82). Hinks JA; Evans MCW; De Miguel Y; Sartori AA; Jiricny J; Pearl LH An Iron-Sulfur Cluster in the Family 4 Uracil-DNA Glycosylases. J. Biol. Chem 2002, 277 (19), 16936–16940. [PubMed: 11877410]

(83). Weiner BE; Huang H; Dattilo BM; Nilges MJ; Fanning E; Chazin WJ An Iron-Sulfur Cluster in the C-Terminal Domain of the P58 Subunit of Human DNA Primase. J. Biol. Chem 2007, 282 (46), 33444–33451. [PubMed: 17893144]

(84). Biochemistry, Biosynthesis and Human Diseases, Vol. 2; Rouault TA, Ed.; De Gruyter: Berlin, Boston, 2017 DOI: 10.1515/9783110479850.

(85). Oberpichler I; Pierik AJ; Wesslowski J; Pokorny R; Rosen R; Vugman M; Zhang F; Neubauer O; Ron EZ; Batschauer A; Lamparter T A Photolyase-like Protein from Agrobacterium Tumefaciens with an Iron-Sulfur Cluster. PLoS One 2011, 6 (10). e26775. [PubMed: 22066008]

(86). Holm RH; Kennepohl P; Solomon EI Structural and Functional Aspects of Metal Sites in Biology. Chem. Rev 1996, 96 (7), 2239–2314. [PubMed: 11848828]

(87). Arnold AR; Zhou A; Barton JK Characterization of the DNA-Mediated Oxidation of Dps, A Bacterial Ferritin. J. Am. Chem. Soc 2016, 138 (35), 11290–11298. [PubMed: 27571139]

(88). Hagen WR EPR Spectroscopy as a Probe of Metal Centres in Biological Systems. Dalt. Trans 2006, No. 37, 4415–4434.

(89). Crack JC; Green J; Thomson AJ; Brun NEL Iron-Sulfur Clusters as Biological Sensors: The Chemistry of Reactions with Molecular Oxygen and Nitric Oxide. Acc. Chem. Res 2014, 47 (10), 3196–3205. [PubMed: 25262769]

(90). Ezraty B; Gennaris A; Barras F; Collet JF Oxidative Stress, Protein Damage and Repair in Bacteria. Nat. Rev. Microbiol 2017, 15 (7), 385–396. [PubMed: 28420885]

(91). Imlay JA Iron-Sulphur Clusters and the Problem with Oxygen. Mol. Microbiol 2006, 59 (4), 1073–1082. [PubMed: 16430685]

(92). Kuo CF; McRee DE; Fisher CL; O'Handley SF; Cunningham RP; Tainer JA Atomic Structure of the DNA Repair [4Fe-4S] Enzyme Endonuclease III. Science 1992, 258 (5081), 434–440. [PubMed: 1411536]

(93). Fromme JC; Banerjee A; Huang SJ; Verdine GL Structural Basis for Removal of Adenine Mispaired with 8-Oxoguanine by MutY Adenine DNA Glycosylase. Nature 2004, 427, 652. [PubMed: 14961129]

(94). Fromme JC; Verdine GL Structure of a Trapped Endonuclease III-DNA Covalent Intermediate. EMBO J. 2003, 22 (13), 3461–3471. [PubMed: 12840008]

(95). Grabarczyk DB; Ash PA; Myers WK; Dodd EL; Vincent KA Dioxygen Controls the Nitrosylation Reactions of a Protein-Bound [4Fe4S] Cluster. Dalton Trans. 2019, 48 (37).13960. [PubMed: 31497816]

(96). Van Der Veen S; Tang CM The BER Necessities: The Repair of DNA Damage in Human-Adapted Bacterial Pathogens. Nat. Rev. Microbiol 2015, 13 (2), 83–94. [PubMed: 25578955]

(97). Hardy PO; Chaconas G The Nucleotide Excision Repair System of Borrelia Burgdorferi Is the Sole Pathway Involved in Repair of DNA Damage by UV Light. J. Bacteriol 2013, 195 (10), 2220–2231. [PubMed: 23475971]

(98). DellaVecchia MJ; Croteau DL; Skorvaga M; Dezhurov SV; Lavrik OI; Van Houten B Analyzing the Handoff of DNA from UvrA to UvrB Utilizing DNA-Protein Photoaffinity Labeling. J. Biol. Chem 2004, 279 (43), 45245–45256. [PubMed: 15308661]

(99). Vaisman A; McDonald JP; Huston D; Kuban W; Liu L; Van Houten B; Woodgate R Removal of Misincorporated Ribonucleotides from Prokaryotic Genomes: An Unexpected Role for Nucleotide Excision Repair. PLoS Genet. 2013, 9 (11).e1003878. [PubMed: 24244177]

(100). Grodick MA DNA-Mediated Charge Transport Signaling within the Cell. Ph.D. Dissertation, California Institute of Technology, Pasadena, CA, 7 1, 2015 DOI: 10.7907/Z9F769GX.

(101). Minko IG; Kurtz AJ; Croteau DL; Van Houten B; Harris TM; Lloyd RS Initiation of Repair of DNA - Polypeptide Cross-Links by the UvrABC Nuclease. Biochemistry 2005, 44 (8), 3000–3009. [PubMed: 15723543]

(102). Truglio JJ; Karakas E; Rhau B; Wang H; Dellavecchia MJ; Van Houten B; Kisker C Structural Basis for DNA Recognition and Processing by UvrB. Nat. Struct. Mol. Biol 2006, 13 (4), 360–364. [PubMed: 16532007]

(103). Karakas E; Truglio JJ; Croteau D; Rhau B; Wang L; Van Houten B; Kisker C Structure of the C-Terminal Half of UvrC Reveals an RNase H Endonuclease Domain with an Argonaute-like Catalytic Triad. EMBO J. 2007, 26 (2), 613–622. [PubMed: 17245438]

(104). Golinelli MP; Chmiel NH; David SS Site-Directed Mutagenesis of the Cysteine Ligands to the [4Fe-4S] Cluster of Escherichia Coli MutY. Biochemistry 1999, 38 (22), 6997–7007. [PubMed: 10353811]

(105). ter Beek J; Parkash V; Bylund GO; Osterman P; Sauer-Eriksson AE; Johansson E Structural Evidence for an Essential Fe–S Cluster in the Catalytic Core Domain of DNA Polymerase ϵ. Nucleic Acids Res. 2019, 47 (11), 5712–5722. [PubMed: 30968138]

(106). Schaefer KN; Barton JK DNA-Mediated Oxidation of P53. Biochemistry 2014, 53 (21), 3467–3475. [PubMed: 24853816]

(107). Schaefer KN; Geil WM; Sweredoski MJ; Moradian A; Hess S; Barton JK Oxidation of P53 through DNA Charge Transport Involves a Network of Disulfides within the DNA-Binding Domain. Biochemistry 2015, 54 (3), 932–941. [PubMed: 25584637]

(108). Yeung AT; Mattes WB; Grossman L Protein Complexes Formed during the Incision Reaction Catalyzed by the Escherichia Coli UvrABC Endonuclease. Nucleic Acids Res. 1986, 14 (6), 2567–2582. [PubMed: 3960727]

(109). Van Houten B; Gamper H; Sancar A; Hearst JE DNase I Footprint of ABC Excinuclease. J. Biol. Chem 1987, 262 (27), 13180–13187. [PubMed: 3308871]

(110). Visse R; De Ruijter M; Moolenaar GF; Van de Putte P Analysis of UvrABC Endonuclease Reaction Intermediates on Cisplatin-Damaged DNA Using Mobility Shift Gel Electrophoresis. J. Biol. Chem 1992, 267 (10), 6736–6742. [PubMed: 1551881]

(111). Moolenaar GF; Bazuine M; Van Knippenberg IC; Visse R; Goosen N Characterization of the Escherichia Coli Damage-Independent UvrBC Endonuclease Activity. J. Biol. Chem 1998, 273 (52), 34896–34903. [PubMed: 9857018]

(112). Singh S; Folkers GE; Bonvin AMJJ; Boelens R; Wechselberger R; Niztayev A; Kaptein R Solution Structure and DNA-Binding Properties of the C-Terminal Domain of UvrC from E. Coli. EMBO J. 2002, 21 (22), 6257–6266. [PubMed: 12426397]

(113). Truglio JJ; Rhau B; Croteau DL; Wang L; Skorvaga M; Karakas E; DellaVecchia MJ; Wang H; Van Houten B; Kisker C Structural Insights into the First Incision Reaction during Nucleotide Excision Repair. EMBO J. 2005, 24 (5), 885–894. [PubMed: 15692561]

(114). Tang MS; Nazimiec M; Ye X; Iyer GH; Eveleigh J; Zheng Y; Zhou W; Tang YY Two Forms of UvrC Protein with Different Double-Stranded DNA Binding Affinities. J. Biol. Chem 2001, 276 (6), 3904–3910. [PubMed: 11056168]

(115). Hughes CD; Wang H; Ghodke H; Simons M; Towheed A; Peng Y; Van Houten B; Kad NM Real-Time Single-Molecule Imaging Reveals a Direct Interaction between UvrC and UvrB on DNA Tightropes. Nucleic Acids Res. 2013, 41 (9), 4901–4912. [PubMed: 23511970]

(116). Wirth N; Gross J; Roth HM; Buechner CN; Kisker C; Tessmer I Conservation and Divergence in Nucleotide Excision Repair Lesion Recognition. J. Biol. Chem 2016, 291 (36), 18932–18946. [PubMed: 27405761]

(117). Orren DK; Sancar A The (A)BC Excinuclease of Escherichia Coli Has Only the UvrB and UvrC Subunits in the Incision Complex. Proc. Natl. Acad. Sci. U. S. A 1989, 86 (14), 5237–5241. [PubMed: 2546148]

(118). Zou Y; Walker R; Bassett H; Geacintov NE; Van Houten B Formation of DNA Repair Intermediates and Incision by the ATP-Dependent UvrB-UvrC Endonuclease. J. Biol. Chem 1997, 272 (8), 4820–4827. [PubMed: 9030538]

(119). Jaciuk M; Nowak E; Skowronek K; Tañska A; Nowotny M Structure of UvrA Nucleotide Excision Repair Protein in Complex with Modified DNA. Nat. Struct. Mol. Biol 2011, 18 (2), 191–198. [PubMed: 21240268]

(120). Caron PR; Grossman L Incision of Damaged versus Nondamaged DNA by the Escherichia Coli Uvrabc Proteins. Nucleic Acids Res. 1988, 16 (16), 7855–7865. [PubMed: 2843804]

(121). Moolenaar GF; Höglund L; Goosen N Clue to Damage Recognition by UvrB: Residues in the β-Hairpin Structure Prevent Binding to Non-Damaged DNA. EMBO J. 2001, 20 (21), 6140–6149. [PubMed: 11689453]

(122). Skorvaga M; Theis K; Mandavilli BS; Kisker C; Van Houten B The β-Hairpin Motif of UvrB Is Essential for DNA Binding, Damage Processing, and UvrC-Mediated Incisions. J. Biol. Chem 2002, 277 (2), 1553–1559. [PubMed: 11687584]

(123). Jain R; Vanamee ES; Dzikovski BG; Buku A; Johnson RE; Prakash L; Prakash S; Aggarwal AK An Iron-Sulfur Cluster in the Polymerase Domain of Yeast DNA Polymerase ε. J. Mol. Biol 2014, 426 (2), 301–308. [PubMed: 24144619]

(124). Grodick MA; Muren NB; Barton JK DNA Charge Transport within the Cell. Biochemistry 2015, 54 (4), 962–973. [PubMed: 25606780]

(125). Arnold AR; Grodick MA; Barton JK DNA Charge Transport: From Chemical Principles to the Cell. Cell Chem. Biol 2016, 23 (1), 183. [PubMed: 26933744]

(126). Boal AK; Barton JK Electrochemical Detection of Lesions in DNA. Bioconjugate Chem. 2005, 16 (2), 312–321.

(127). Pheeney CG; Arnold AR; Grodick MA; Barton JK Multiplexed Electrochemistry of DNA-Bound Metalloproteins. J. Am. Chem. Soc 2013, 135 (32), 11869–11878. [PubMed: 23899026]

(128). Zhou A Investigations of DNA-Mediated Redox Signaling Between E.coli DNA Repair Pathways. Ph.D. Dissertation, California Institute of Technology, Pasadena, CA, 7 23, 2018 DOI: 10.7907/G7NF-S349.

(129). Moolenaar GF; Van Rossum-Fikkert S; Van Kesteren M; Goosen NC A Second Endonuclease Involved in Escherichia Coli Nucleotide Excision Repair. Proc. Natl. Acad. Sci. U. S. A 2002, 99 (3), 1467–1472. [PubMed: 11818552]

(130). Perera AV; Mendenhall JB; Courcelle CT; Courcelle J Cho Endonuclease Functions during DNA Interstrand Cross-Link Repair in Escherichia Coli. J. Bacteriol 2016, 198 (22), 3099–3108. [PubMed: 27573016]

(131). White MF; Allers T DNA Repair in the Archaea-an Emerging Picture. FEMS Microbiol. Rev 2018, 42 (4), 514–526. [PubMed: 29741625]

(132). Yan A; Kiley PJ Chapter 42 Techniques to Isolate O2-Sensitive Proteins. [4Fe-4S]-FNR as an Example. Methods Enzymol. 2009, 463, 787–805. [PubMed: 19892202]

(133). Senda M; Senda T Anaerobic Crystallization of Proteins. Biophys. Rev 2018, 10 (2), 183–189. [PubMed: 29198081]

(134). Lu Z; Sethu R; Imlay JA Endogenous Superoxide Is a Key Effector of the Oxygen Sensitivity of a Model Obligate Anaerobe. Proc. Natl. Acad. Sci. U. S. A 2018, 115 (14), E3266–E3275. [PubMed: 29559534]

(135). Moolenaar GF; Monaco V; Van Der Marel GA; Van Boom JH; Visse R; Goosen N The Effect of the DNA Flanking the Lesion on Formation of the UvrB-DNA Preincision Complex. Mechanism for the UvrA-Mediated Loading of UvrB onto a DNA Damaged Site. J. Biol. Chem 2000, 275 (11), 8038–8043. [PubMed: 10713124]

(136). Slinker JD; Muren NB; Gorodetsky AA; Barton JK Multiplexed DNA-Modified Electrodes. J. Am. Chem. Soc 2010, 132 (8), 2769–2774. [PubMed: 20131780]

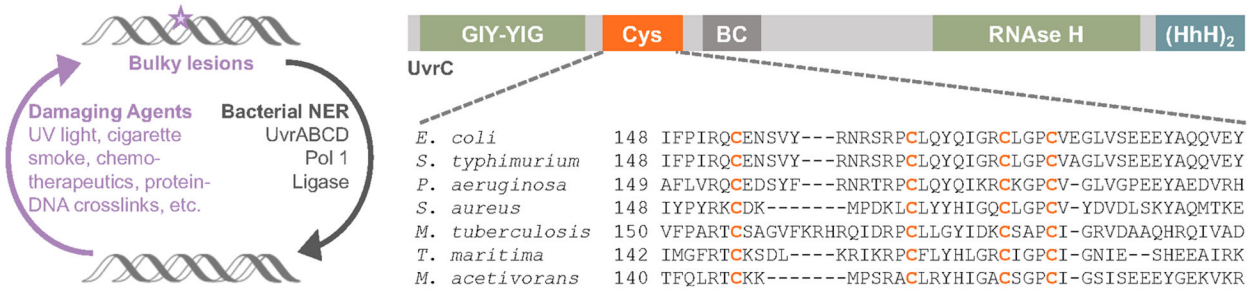

Figure 1.

Sequence of UvrC. The excision nuclease in bacterial nucleotide excision repair (NER), contains a putative [4Fe4S] cluster coordination site. (Left) DNA damage caused by agents that generate bulky lesions (light purple) are resolved by bacterial NER machinery through excision and removal of damaged oligomers (UvrABCD) followed by patching by Pol 1 and Ligase (gray). (Right) Four conserved cysteine residues contained in the N-terminal region of UvrC. (Right, Top) Shown is a schematic representation the GIY-YIG endonuclease (3′ incision, green), cysteine rich (Cys, orange), UvrBC interacting (BC, purple), RNase H endonuclease (5′ incision, green), and helix-turn-helix ($(HhH)_2$ teal) domains of UvrC. (Right, Bottom) Within the N-terminal, cysteine-rich region (shown are residues 148 to 194), Cys154, Cys166, Cys174, Cys178 (*E. coli* numbering) are highly conserved and atypically spaced in bacterial and several archaeal species.

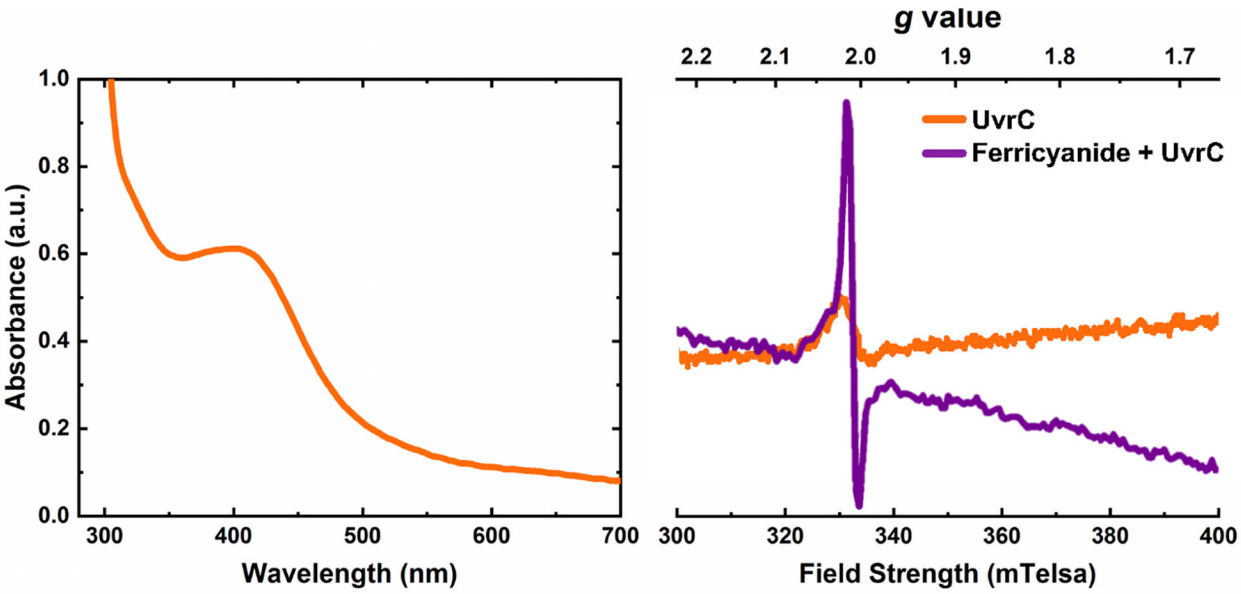

Figure 2.

UvrC coordinates a [4Fe4S] cluster. (Left) UV–visible absorbance spectrum for purified UvrC shows a broad and shallow absorption band centered at 410 nm, which is characteristic of [4Fe4S] clusters. The concentration of cluster-loaded protein shown was 35 μM (60% loading) with ~3 Fe per protein. (Right) Using X band EPR spectroscopy, a small signal was observed for UvrC (orange) at $g = 2.01$, which is attributed to a small percentage of the protein population in the $[3Fe4S]^{1+}$ state. A large and sharp signal was observed in the presence of ferricyanide (purple), at $g = 2.01$. This signal is attributed to the transformation of oxidized $[4Fe4S]^{3+}$ species to the $[3Fe4S]^{1+}$ species. All spectra were taken in buffer containing 25 mM Tris, 0.5 M KCl, and 20% glycerol (v/v) at a pH of 7.5 (UvrC buffer). EPR conditions: 9.37 GHz, 10 K, 16 mW microwave power.

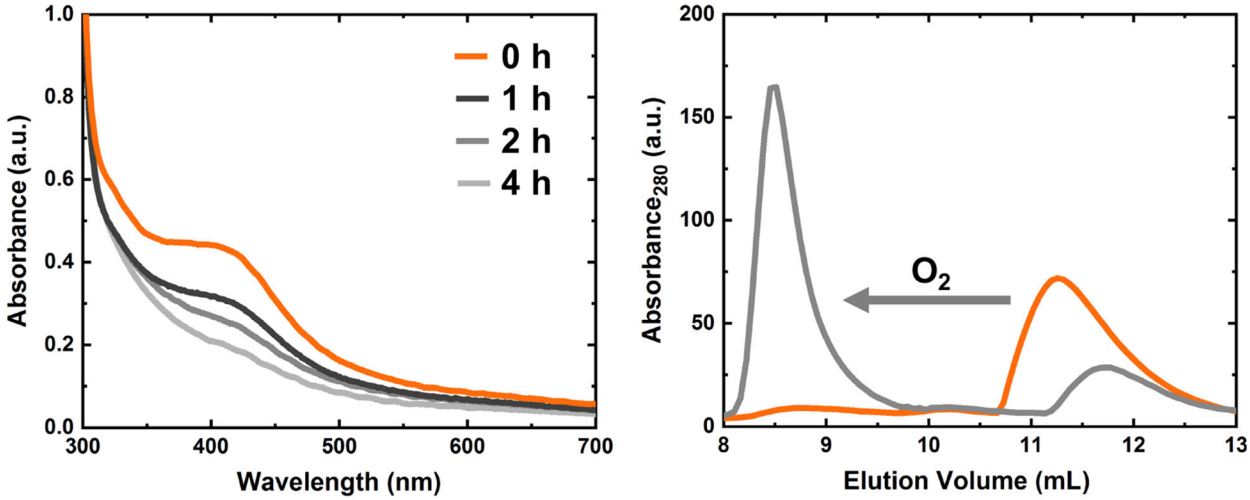

Figure 3.

UvrC-bound [4Fe4S] cluster undergoes degradation in the presence O_2. (Left) Incubation of UvrC at 37 °C in aerobic UvrC buffer (25 mM Tris-HCl, 0.5 M KCl, 20% v/v glycerol) resulted in the disappearance of the absorption band at 410 nm. Incubation for 1 h (the time scale of an activity assay) led to 20% degradation. (Right) Holo-UvrC was examined by size exclusion chromatography in degassed buffer at room temperature. Holoenzyme (orange trace) eluted at a volume consistent with a dimer (see also Figure S4). Apoprotein (gray trace) arising from oxidative degradation eluted at the void volume, indicating the apoprotein had formed species >600 kDa.

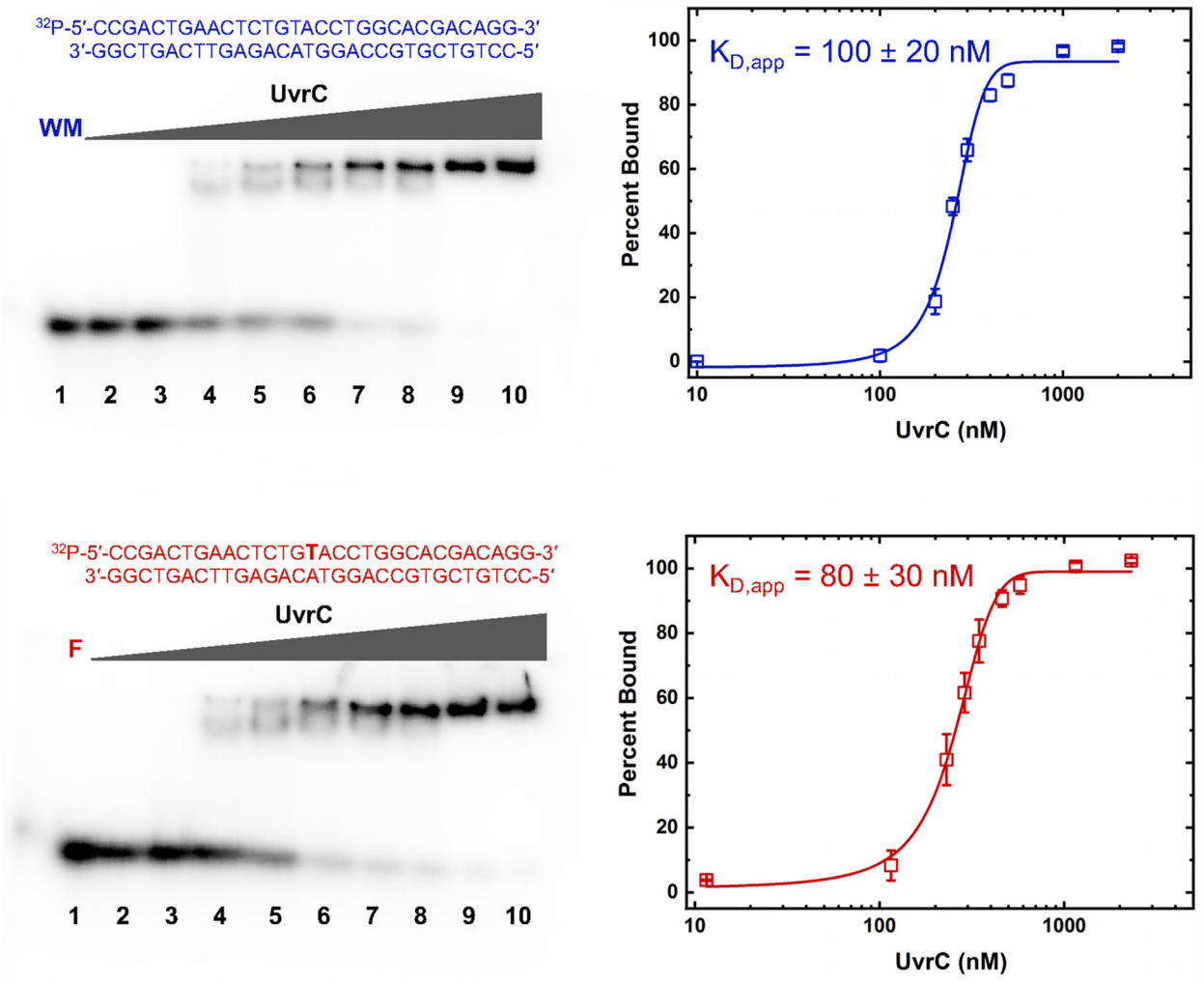

Figure 4.

UvrC forms a complex with DNA substrates. UvrC was incubated with 30 base pair DNA substrates in degassed UvrC buffer (25 mM Tris-HCl, 0.5 M KCl, 20% v/v glycerol). Free and complexed DNA were separated by native gel electrophoresis using degassed running buffer (25 mM Tris-HCl, 192 mM glycine, pH 8.3) in an anaerobic chamber in an atmosphere of N_2 with 2–4% H_2 at room temperature. Data from the electrophoretic mobility shift assays indicate that UvrC forms a complex with both well-matched (WM) duplex DNA and a fluorescein-modified (F) substrate at a high affinity. Lane 1: DNA only (100 nM). Lanes 2–10: 10 nM to 2 μM UvrC by cluster with a constant duplex concentration of 100 nM. For each DNA substrate, binding data from three independent trials were individually fit using a Hill function and then the apparent dissociation constants were averaged (reported with the standard error of the mean).

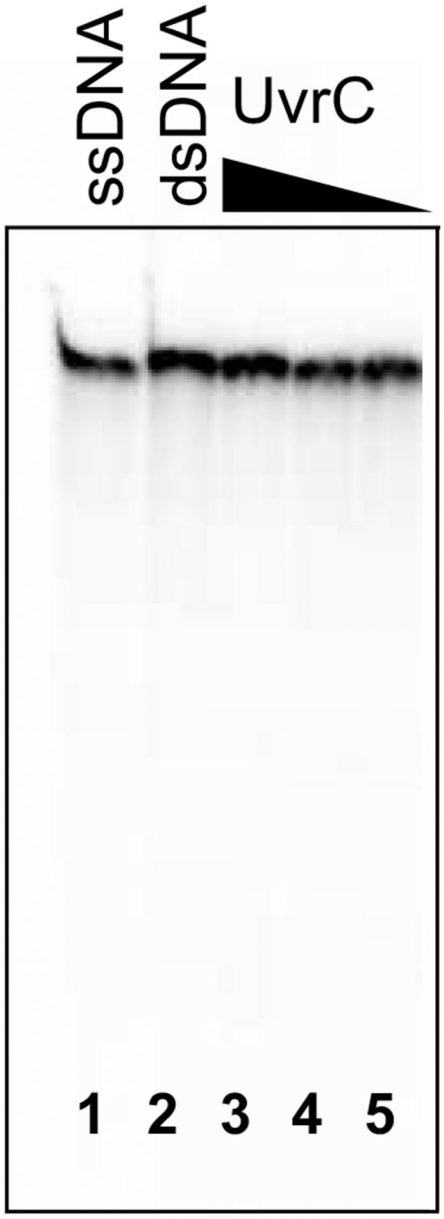

Figure 5.

UvrC in the holo form alone is not enzymatically active on a damaged substrate. UvrC was incubated with the fluorescein-modified substrate (3 μM) at 37 °C in activity buffer containing 25 mM Tris, 0.1 M KCl, and 20% glycerol (v/v) at a pH of 7.5 in the presence of 10 mM Mg^{2+}, 10 mM ATP, and 1 mM DTT under anaerobic conditions. On a denaturing 20% urea gel, incision of the damaged strand was not observed. Lane 1: ssDNA; Lane 2: dsDNA; Lanes 3–5: 1 μM–10 nM UvrC.

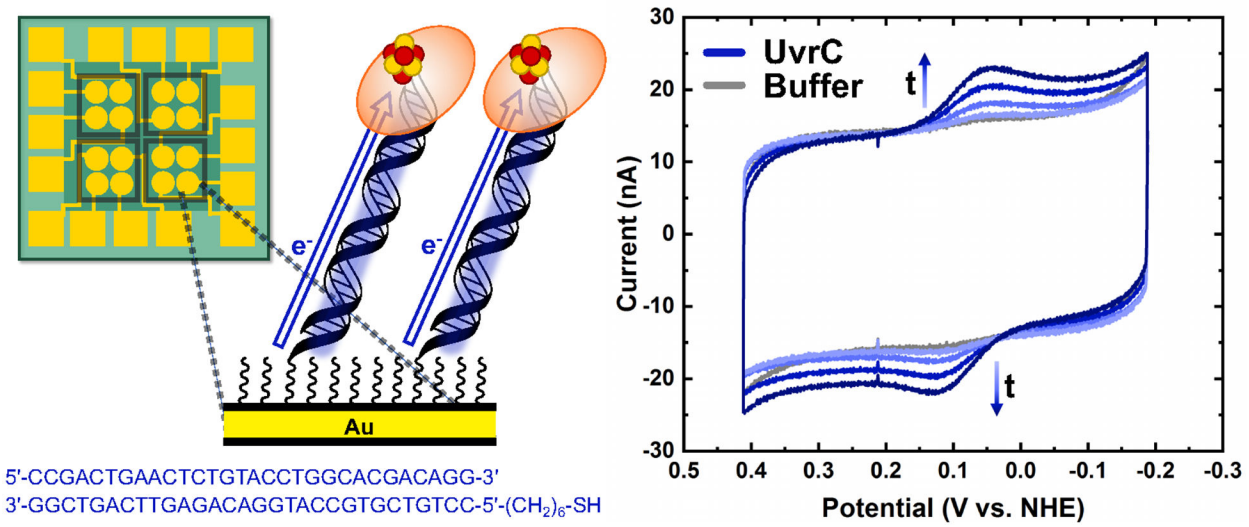

Figure 6.

UvrC participates in DNA charge transport chemistry. (Left) Shown is a schematic of DNA-modified electrodes on multiplex chips. DNA duplexes are formed in monolayers through an alkane-thiol linker on gold multiplex chips with 16 independently addressable electrodes.[12] (Right) All measurements were taken in an anaerobic chamber in degassed electrochemistry buffer (25 mM Tris-HCl, 0.25 M KCl, 20% glycerol (v/v), 4 mM spermidine, and 0.5 mM EDTA at pH 7.5). On DNA-modified gold electrodes, UvrC (5 μM, 400 μL) is redox active at physiological potentials, exhibiting a reversible signal with a midpoint potential of 90 mV ± 0.03 vs NHE. The initial signal (light blue) increases over time (1–3 h) as protein diffuses to the monolayer surface. UvrC and all other [4Fe4S] repair proteins from *E. coli*, EndoIII, MutY, and DinG share a DNA-bound potential which can facilitate redox sensing and signaling among different repair pathways *in vivo*.

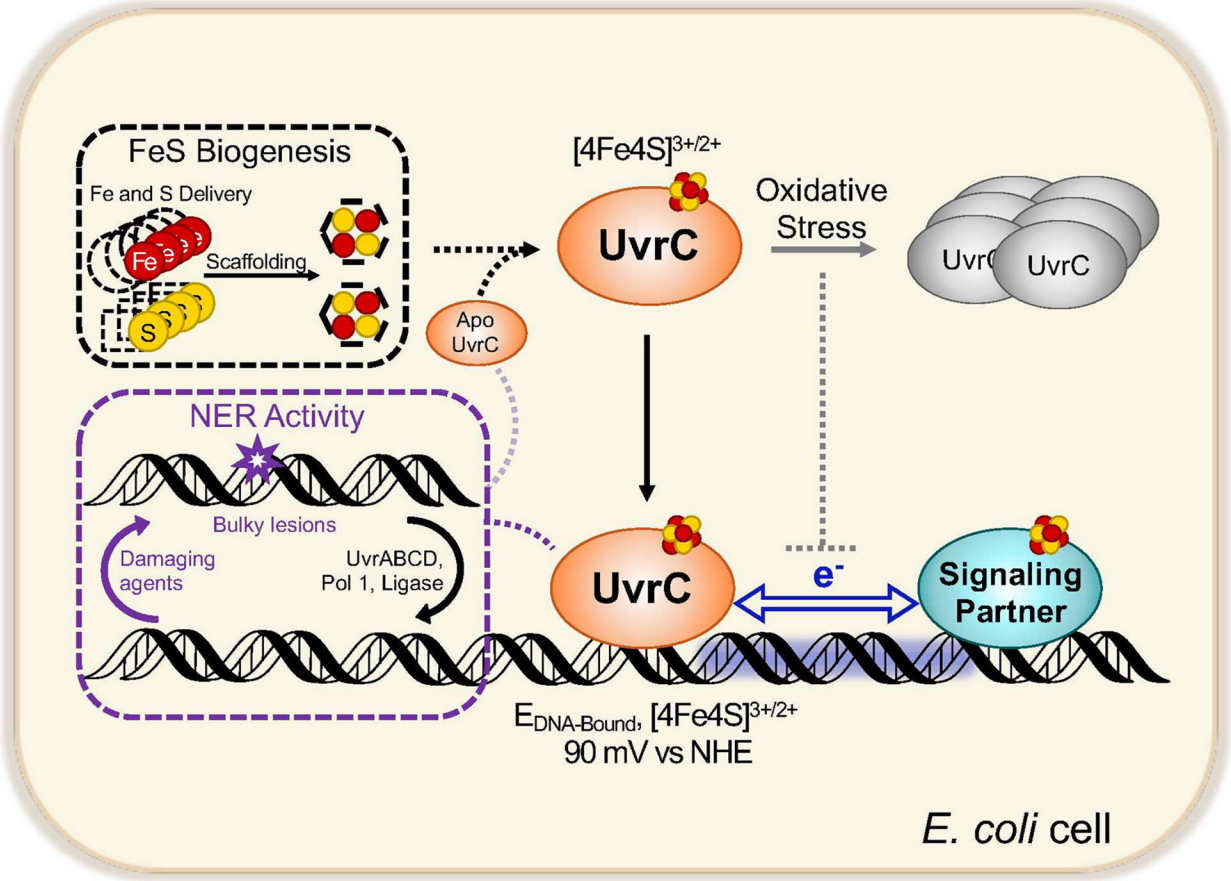

Figure 7.

Examination of UvrC in its holo form is likely to uncover many crucial details regarding the activity of UvrC *in vivo*. Connections between FeS biogenesis machinery and the NER pathway (dashed, black square and dashed, purple square), cellular functions of apo (orange oval), holo (orange oval and cofactor) and aggregated UvrC (gray ovals), the role of O_2 sensitivity (solid gray arrow), and DNA-mediated redox signaling with other repair pathways (solid blue, double headed arrow) remain to be explored.